

The authors thank the editor and referees to review our manuscript and particularly for the valuable comments and suggestions that are very helpful in improving the manuscript. We provide below point-by-point responses to those comments. We also have made most of the changes suggested by the referees in the revised manuscript.

## **Referee #1**

In this study, Huang et al. used an aerosol chemical species monitor (ACSM) and an aethalometer to characterize the organic aerosol (OA) in wintertime Beijing. Positive matrix factorization (PMF) was applied to resolve the sources and processes for OA. The effect of RH on the mass concentration, the mass fraction, and the growth rate of various components in PM<sub>1</sub> was analyzed. OA was found to dominate the components under both high-RH and low-RH pollution periods. But the change of sulfate and nitrate showed opposite RH-dependence. The results demonstrated the importance of photochemical oxidation and aqueous-phase processes on the formation of secondary aerosol during haze episodes. It could be helpful for understanding the haze formation in wintertime Beijing. Overall, the results are well presented. I recommend the manuscript be considered for publication after following comments being fully addressed.

(1) First of all, the motivation of research should be explained more clearly in the introduction section.

**Response:** We thank the referee's suggestion. In the revised manuscript lines 103-107, we have now added the following description: "Despite the observations of large production of secondary aerosol during haze events, the formation mechanisms are not yet well understood. Specifically, more studies are needed to elucidate the relative importance of photochemical oxidation versus aqueous-phase processes on the formation of secondary aerosol during wintertime haze episodes of different meteorological conditions".

(2) The criteria to distinguish clean day and polluted days, as well as low RH and high RH seem a little bit arbitrary. The selection of the concentration threshold of PM<sub>1</sub> for discriminating the clean and pollution period, as well as RH, should be explained.

**Response:** As shown in Figure 1, the clean and pollution episodes occurred alternately during the measurement period, and the PM<sub>1</sub> concentration was usually lower than 20  $\mu\text{g m}^{-3}$  during clean episodes and higher than 100  $\mu\text{g m}^{-3}$  during polluted episodes. Thus, we divided the measurements into clean period and pollution period using the criteria of 20  $\mu\text{g m}^{-3}$  and 100  $\mu\text{g m}^{-3}$ , respectively. Furthermore, during the pollution period, RH varied from 15% to 95% with an average value of 46% ( $\approx 50\%$ ) and a median value of 43%, thus we used 50% as the criterion to further divide the pollution period into low-RH pollution days (RH <50%) and high-RH pollution days (RH >50%).

In lines 213-215 in the revised manuscript, we have now added "The clean and pollution episodes occurred alternately during the measurement period, and the PM<sub>1</sub> concentration was usually lower than 20  $\mu\text{g m}^{-3}$  during clean episodes and higher than 100  $\mu\text{g m}^{-3}$  during pollution episodes. As such...".

And in lines 220-221, we have added “During the polluted period, RH varied from 15% to 95% with an average value of 46% and a median value of 43%. To investigate...”.

(3) It was noted that in Figure 4 where OOA reached a peak value at about 20:00 LT. The authors may give an interpretation about this phenomenon. Also, what is the reason that OOA increased more quickly under low RH condition than under high RH conditions?

**Response:** In the section 3.2, we discuss that the diurnal cycle of OOA shows an increase from about 6:00 to 20:00 LT, indicating the contribution from photochemical production. The peak value at about 20:00 LT may be due to the accumulation of OOA formed from photochemical production. Meanwhile, as discussed in section 3.4, photochemical production contributed dominantly to OOA. The  $O_x$  concentration during low-RH pollution days (59.8 ppb) was higher than that during high-RH pollution days (47.8 ppb) and clean days (39.2 ppb). With the higher  $O_x$  concentration (as a surrogate of oxidant level) under low-RH conditions, the daytime formation of OOA was more efficient and the growth rate was higher during those low-RH pollution days than those during high-RH pollution days and clean days.

In line 328 of the revised manuscript, we added “...photochemical production and accumulation of OOA”.

(4) Lines 328-332: Why the concentration of  $O_x$  ( $=O_3+N_2O$ ) was lower than that of  $NO_2$ ? Please check carefully. Meanwhile, the mass fraction of some species (e.g.,  $Cl^-$ ) was missing in Fig. 5.

**Response:** Apologies for the typos. We double check our data, and it now reads: “ $NO_2$  increased accordingly from 16.7 ppb during clean periods to 42.2 ppb during high-RH pollution periods and to 55.4 ppb during low-RH pollution periods”. We have changed the  $NO_2$  values in Table1 accordingly. The missing mass fractions for some species are also added in Figure 5.

(5) Lines 335-337: I don’t think there was obvious difference in the mass fraction of nitrate in two types of pollution periods (14 % vs. 15 %). And references need to be cited in Line 337. In addition, this sentence is too hard to read. Rewrite it!

**Response:** We thank the referee for pointing this out. We have made the change and it now reads “We observed similar contributions from nitrate during low-RH pollution periods and high-RH pollution periods, while a much larger contribution from sulfate during high-RH pollution periods than during low-RH pollution periods because of enhanced formation from aqueous-phase processes”.

Meanwhile, references were added in line 363, and it now reads “...indicating the importance of residential coal combustion emissions during haze pollution in wintertime Beijing (Elser et al., 2016; Li et al., 2017).”.

(6) Lines 391-395: Was P3 assigned to high-RH or low-RH pollution during the analyses of sulfate and OA?

**Response:** P3 was assigned to high-RH pollution episode during the analyses of sulfate

and OOA. We made change in lines 415-416 and it now reads “OOA also showed a much higher contribution to OA during high-RH pollution events (62% for P6 and 50% for P7) than during low-RH pollution events (P1, P2, P4 and P5, 20-31%)”.

(7) Line 423. The measurement of SO<sub>2</sub> was not described in the Section 2.1 Site description and instrumentation.

**Response:** Thanks for the referee’s reminder. In the revised manuscript lines 136-138, we have now added “The gaseous species including O<sub>3</sub>, NO<sub>x</sub>, and SO<sub>2</sub> were measured by a Thermo Scientific Model 49i ozone analyzer, a Thermo Scientific Model 42i NO–NO<sub>2</sub>–NO<sub>x</sub> analyzer, and an Ecotech EC 9850 sulfur dioxide analyzer, respectively”.

(8) Conclusion. I think a brief description of atmospheric implications should be included in this section.

**Response:** In the revised manuscript (lines 478-481), we have now added the following discussion “These results provide insights into the relative importance of photochemical oxidation and aqueous-phase processes for secondary aerosol formation during haze pollution, demonstrating the significance of meteorological conditions in the formation of secondary aerosol.”

## Referee #2

This manuscript presents the comparisons of PM<sub>1</sub> species and organic aerosol (OA) sources/processes during winter in Beijing for clean and pollution periods, with a particular focus on the effect of relative humidity (RH) on secondary aerosol formation. The comparisons were made through mass concentration, mass fraction, and growth rate. It is found that OA dominated the PM<sub>1</sub> mass under both low-RH and high-RH pollution conditions. However, sulfate was found to increase during high-RH pollution periods and nitrate increased during low-RH pollution periods. Oxygenated OA (OOA) showed higher growth rate during low-RH pollution period than during high-RH pollution period. These results provide insights into the relative importance of photochemical oxidation vs. aqueous-phase processes for secondary aerosol formation under different meteorological conditions. It is a useful addition to the literature for understanding the haze formation in Beijing. The manuscript is well written, and results are discussed logically. I recommend publication in ACP after a few minor points are addressed.

(1) In section 2.2.3, organics was not considered in the ALWC calculation using the ISORROPIA-II model. Please provide an explanation.

**Response:** We thank the reviewer for pointing this out. We calculated the ALWC using the ISORROPIA-II model, which simulates the thermodynamic equilibrium of the NH<sub>4</sub><sup>+</sup>–SO<sub>4</sub><sup>2-</sup>–NO<sub>3</sub><sup>-</sup>–Cl–H<sub>2</sub>O system and does not consider the organics contribution. To evaluate this uncertainty, we further calculate the contribution of organics to ALWC following the

approach in Guo et al (2015) and Cheng et al (2016):

$$W_{\text{org}} = \frac{\text{OM}}{\rho_{\text{org}}} \cdot \rho_{\text{w}} \cdot \frac{\kappa_{\text{org}}}{(100\%/\text{RH} - 1)}$$

where OM is the mass concentration of organics,  $\rho_{\text{w}}$  is the density of water and  $\rho_{\text{org}}$  is the density of organics ( $\rho_{\text{org}} = 1.4 \times 10^3 \text{ kg m}^{-3}$ , Cerully et al., 2014).  $\kappa_{\text{org}}$  is the hygroscopicity parameter of organic aerosol composition. We adopted a  $\kappa_{\text{org}}$  value of 0.06 based on previous cloud condensation nuclei measurements in Beijing (Gunthe et al., 2011).

The calculated results showed that the average contribution of organics to the total ALWC was 18%, suggesting that inorganic species were the dominant hygroscopic species and organics had a minor contribution to ALWC.

In the revised manuscript, we added the following description in section 2.3.3:

“Meanwhile, the contribution of organics to ALWC ( $\text{ALWC}_0$ ) was also calculated using the following equation (Guo et al., 2015; Cheng et al., 2016):

$$W_{\text{org}} = \frac{\text{OM}}{\rho_{\text{org}}} \cdot \rho_{\text{w}} \cdot \frac{\kappa_{\text{org}}}{(100\%/\text{RH} - 1)}$$

where OM is the mass concentration of organics,  $\rho_{\text{w}}$  is the density of water and  $\rho_{\text{org}}$  is the density of organics ( $\rho_{\text{org}} = 1.4 \times 10^3 \text{ kg m}^{-3}$ , Cerully et al., 2014).  $\kappa_{\text{org}}$  is the hygroscopicity parameter of organic aerosol composition. We adopted a  $\kappa_{\text{org}}$  value of 0.06 based on previous cloud condensation nuclei measurements in Beijing (Gunthe et al., 2011).”

Figure 7 was also updated accordingly.

(2) Page 6, line 203-205, the authors divided the pollution period into low-RH pollution days ( $\text{RH} < 50\%$ ) and high-RH pollution days ( $\text{RH} > 50\%$ ). What is the criterion for this definition of low- and high-RH?

**Response:** As discussed in response to referee #1, during the polluted period, RH varied from 15% to 95% with an average value of 46% ( $\approx 50\%$ ) and a median value of 43%. Thus, we used 50% as the criterion to further divide the pollution period into low-RH pollution days ( $\text{RH} < 50\%$ ) and high-RH pollution days ( $\text{RH} > 50\%$ ). If 60% is used as a cutting point, the data points (78) in  $\text{RH} > 60\%$  are much less than those in  $\text{RH} < 60\%$  (282), which may be not proper for statistical comparison.

In the revised manuscript lines 220-221, we have added “During the polluted period, RH varied from 15% to 95% with an average value of 46% and a median value of 43%. To investigated...”.

(3) Page 8, line 303, change “OOA is correlated well with nitrate ( $R^2=0.89$ ). and the diurnal cycle : : : : :” to “OOA is correlated well with nitrate ( $R^2=0.89$ ), and the diurnal cycle : : : : :”.

**Response:** Change made.

(4) Page 9, line 330-334. “: : : : :We observed a much larger contribution from nitrate

during low-RH pollution periods than during high-RH pollution periods: : : :” This is not well supported as both the mass concentration and fraction of nitrate are similar. Please check it carefully.

**Response:** We thank the referee for pointing this out. In the revised manuscript lines 353-358, it now reads “We observed similar contributions from nitrate during low-RH pollution periods and high-RH pollution periods, while a much larger contribution from sulfate during high-RH pollution periods than during low-RH pollution periods because of enhanced formation from aqueous-phase processes”.

(5) In Table 1 and throughout the manuscript, the authors should pay attention to the significant digits which denotes precision of measurements.

**Response:** Thanks. In the revised manuscript, we have now unified the significant digits throughout the manuscript and Table 1.

### Referee #3

This paper focuses on discussing the secondary aerosol formation processes under different RH conditions mainly. It is valuable to understand the aerosol chemistry in Beijing, but I have a few serious concerns on current results and interpretation. See below:

(1) One concern is that the dataset used is relatively old (five years ago). It is therefore not very up-to-date to reflect the real processes in current atmosphere given the concentrations, compositions of PM<sub>1</sub> as well as the precursors might have changed greatly in Beijing. The authors have to comment more on the implications of findings here.

**Response:** We agree with the referee that the concentrations, compositions of PM<sub>1</sub> as well as the precursors might have some changes in recent years. Our measurements were conducted after the implementation of legislative ‘Air Pollution Prevention and Control Action Plan’ in 2013. Therefore, our results show some similar variations on the PM<sub>1</sub> composition when compared to more recent studies, such as the increase of nitrate and decrease of sulfate. Meanwhile, our study focused on the formation mechanisms of secondary aerosol during different meteorological conditions in haze pollution, especially the significant effects of RH, which is still not well elucidated. The results demonstrated the importance of photochemical oxidation and aqueous-phase processes on the formation of secondary aerosol during haze episodes. It could be helpful for understanding the haze formation in wintertime Beijing. Therefore, our study still provides valuable information to the scientific community to improve our understanding of fine PM pollution.

In the revised manuscript, we have now added the following discussion in conclusion: “These results provide insights into the relative importance of photochemical oxidation and aqueous-phase processes for secondary aerosol formation during haze pollution, demonstrating the significance of meteorological conditions in determining the formation of secondary aerosol”.

(2) More details regarding the PMF analyses should be provided. It is not clear why 5-factor solution is optimal, considering that you use ACSM data which had very limited chemical resolution to identify tracer ions. And you used ME-2 technique, which on one hand is better to extract the real factors presenting in your data, but on the other hand, you may presume and artificially identify a factor that might not be real. Justification of the PMF results is essential and why and how the initial profiles of different factors were used are not clear. I feel that current information provided here is not enough.

**Response:** Thanks for the referee's suggestion. We first performed free PMF (unconstrained PMF) runs to identify the main factors. The number of factors was determined by examining three to seven factors, and the factors were identified based on their mass spectral profiles and correlation with external tracers. The five-factor solution (i.e., HOA, COA, CCOA, BBOA, and OOA) was selected because it best explains our data. For the solutions with less than 5 factors, HOA appeared to be mixed with COA while CCOA mixed with BBOA (Fig. S1). However, when the number of factors was increased to 6, the OOA factor split into two OOA factors of similar time series (Fig. S2), suggesting that further separation of the factors does not improve the interpretation of the data. After determining the number of factors (five) using un-constrained PMF runs, we then performed ME-2 runs, which explore the variabilities of certain (mainly primary) factors (i.e., HOA, COA, and BBOA) by constraining their profiles with  $\alpha$  value approach. In a word, the un-constraint PMF helps making sure that the five factors were real (without "forced deconvolution" as in constrained ME-2), while the constrained ME-2 helps refining the contributions from those five factors. Please see Fig. S1-3 and the corresponding discussion in Section 3.2 for further details of the PMF/ME-2.

(3) Calculation of ALWC by using ISORROPIA-II model had uncertainties as it only consider water uptake by inorganic species but organics is dominant your PM1, please comment on this, and discuss the influences on your results.

**Response:** We thank the reviewer for pointing this out. We calculated the ALWC using the ISORROPIA-II model, which simulates the thermodynamic equilibrium of the  $\text{NH}_4^+ - \text{SO}_4^{2-} - \text{NO}_3^- - \text{Cl}^- - \text{H}_2\text{O}$  system and does not consider the organics contribution. To evaluate this uncertainty, we further calculate the contribution of organics to ALWC following the approach in Guo et al (2015) and Cheng et al (2016):

$$W_{\text{org}} = \frac{\text{OM}}{\rho_{\text{org}}} \cdot \rho_w \cdot \frac{\kappa_{\text{org}}}{(100\%/\text{RH} - 1)}$$

where OM is the mass concentration of organics,  $\rho_w$  is the density of water and  $\rho_{\text{org}}$  is the density of organics ( $\rho_{\text{org}} = 1.4 \times 10^3 \text{ kg m}^{-3}$ , Cerully et al., 2014).  $\kappa_{\text{org}}$  is the hygroscopicity parameter of organic aerosol composition. We adopted a  $\kappa_{\text{org}}$  value of 0.06 based on previous cloud condensation nuclei measurements in Beijing (Gunthe et al., 2011).

The calculated results showed the average contribution of organics to the total ALWC was 18%, suggesting that inorganic species were the dominant hygroscopic species and organics had minor contribution to ALWC.



In the revised manuscript, we have added following description in section 2.3.3:  
 “Meanwhile, the contribution of organics to ALWC(ALWC<sub>0</sub>) was also calculated using the following equation (Guo et al., 2015; Cheng et al., 2016):

$$W_{\text{org}} = \frac{\text{OM}}{\rho_{\text{org}}} \cdot \rho_w \cdot \frac{\kappa_{\text{org}}}{(100\%/\text{RH} - 1)}$$

where OM is the mass concentration of organics,  $\rho_w$  is the density of water and  $\rho_{\text{org}}$  is the density of organics ( $\rho_{\text{org}} = 1.4 \times 10^3 \text{ kg m}^{-3}$ , Cerully et al., 2014).  $\kappa_{\text{org}}$  is the hygroscopicity parameter of organic aerosol compositions. We adopted a  $\kappa_{\text{org}}$  value of 0.06 based on previous cloud condensation nuclei measurements in Beijing (Gunthe et al., 2011).”

Also Figure 7 was updated accordingly.

(4) A very serious concern is the large uncertainty of your interpretation. In order to make strong argument regarding the different chemical processes under different RH conditions. You have to eliminate the influences of other meteorological conditions (PBL, wind directions, speeds, and different air masses) on the concentrations, compositions and growth rates you investigated here. Otherwise, you cannot claim that the observed changes were solely due to chemistry. This reviewer see very little discussions regarding this point, and this make the results highly untrustworthy. For example, the calculation of growth rates, such rates is largely not due to chemistry but likely PBL variations, etc. In understand that the authors argue that during pollution period, there was low wind and mainly south/southeasterly wind mainly; this is too general and does not help resolve what I mention here.

**Response:** We agree with the referee that factors, such as PBL height and winds, might complicate the interpretation of chemical processes under different RH conditions. For example, the growth rates of different species might be affected by those factors. Here in this study, however, we did not intend to emphasize on the absolute values of growth rates, which make less sense given the factors mentioned above. Instead, we mostly tried to compare the growth rates of different species (e.g., sulfate and nitrate in lines 243-244) under the same periods, which should share the effects by those factors. When we did compare the growth rates of the same species under different time periods (low-RH and high-RH pollution conditions), as also pointed out by the reviewer, we assumed that the influences from those factors were more or less similar for these two types of pollution conditions. To provide a note of caution, the caveat of this kind of comparison is now added in lines 250-255 in the revised manuscript: “Note that the comparison of growth rates was done under the assumption that chemical processes were the main reason for mass growth, which might not be the case if other factors such as planetary boundary layer height variations dominate. Yet comparison of growth rates of different species in the same time period would not be affected by these factors because those species should share the same effects”.

(5) L199-L201: Table 1 does not provide wind directions as you said.

**Response:** Apologies for the typo. Table 1 has been changed to Fig. 1.

(6) Indeed, similar discussion had been published in a few references cited here, and it seems to be a bit superficial here, especially section 3.4. The authors need to add more discussions, and point out clearly what are the unique and novel findings here from other studies.

**Response:** We agree with the referee that some similar discussion had been published in a few references cited here. However, the causes of fine PM pollution in urban Beijing are still not fully understood, most likely due to the campaign-to-campaign difference in meteorological conditions, emissions, and atmospheric processes. In addition, previous studies usually focused on sources variations or only SIA or SOA formations (Sun et al., 2015; Hu et al., 2016; Hu et al., 2017; Xu et al., 2017). In our study, we focused on the RH effects during haze pollution. The effect of RH on the mass concentration, the mass fraction, and the growth rate of various components in PM<sub>1</sub> was all analyzed. OA was found to dominate the components under both high-RH and low-RH pollution periods. But the change of sulfate and nitrate showed opposite RH-dependence. The results demonstrated the importance of photochemical oxidation and aqueous-phase processes on the formation of secondary aerosol during haze episodes. It could be helpful for understanding the haze formation in wintertime Beijing. Therefore, our study still provides valuable information to the scientific community to improve our understanding of fine PM pollution.

In the revised manuscript, we have now added the following discussion in section 3.4 in lines 436-438: “Meanwhile, the high ratio between NO<sub>3</sub><sup>-</sup> and SO<sub>4</sub><sup>2-</sup> suggest the nitrate production is more efficient than that of sulfate during low-RH pollution period”, and in lines 447-452: “Meanwhile, the O<sub>x</sub> concentration during low-RH pollution days (59.8 ppb) was higher than that during high-RH pollution days (47.8 ppb) and clean days (39.2 ppb). With the higher O<sub>x</sub> concentration (as a surrogate of oxidant level) under low-RH conditions, the daytime formation of OOA was more efficient and the growth rate was higher during those low-RH pollution days than those during high-RH pollution days and clean days”.

And added the following discussion in the conclusion in lines 478-481: “These results provide insights into the relative importance of photochemical oxidation and aqueous-phase processes for secondary aerosol formation during haze pollution, demonstrating the significance of meteorological conditions in determining the formation of secondary aerosol”.

(7) Why you chose 50% RH as a cutting point for low- and high-RH conditions? How about 60%, and how does this choice possibly influence your findings?

**Response:** During the pollution period, RH varied from 15% to 95% with an average value of 46% and a median value of 43%. Thus, we used 50% as the criterion to further divide the pollution period into low-RH pollution days (RH <50%) and high-RH pollution days (RH >50%). If 60% is used as a cutting point, the data points (78) in RH >60% are much less than those in RH <60% (282), which may be not proper for statistical comparison. Meanwhile, this choice has minor influence on our findings. For example, when using 60% RH as the cutting point, Figure R1 (left) and Figure R2 (right) are very similar to those



two figures (Fig. 6 and Fig. 7) in the manuscript. The better correlation between SOR and ALWC in high RH condition and the conclusion of “Aqueous-phase production of  $\text{SO}_4^{2-}$  become important during high RH periods” are still valid. Also, as shown in Figure R1 (left) below, when using 60% RH, some data in 50%~60% shows similar trend with that of  $\text{RH} > 60\%$ , further confirming that 50% RH is a better choice as the cutting point for low- and high-RH pollution conditions.

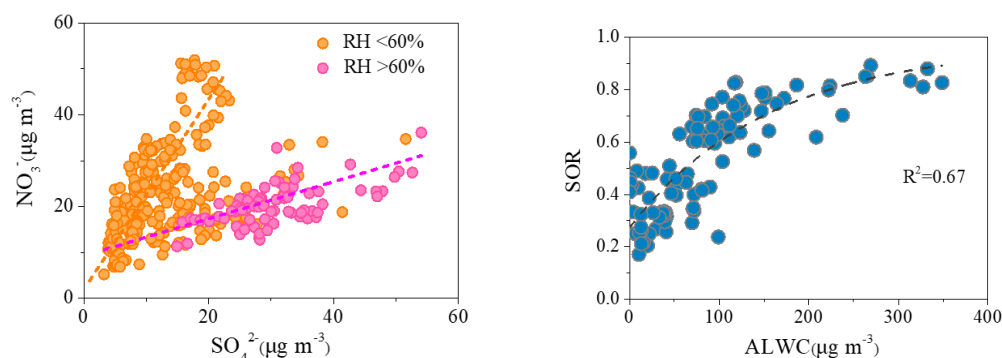


Fig. R1. The relationship between  $\text{SO}_4^{2-}$  and  $\text{NO}_3^-$  during low-RH ( $\text{RH} < 60\%$ ) and high-RH ( $\text{RH} > 60\%$ ) pollution episodes (left).

Fig. R2. The relationship between the sulfate oxidation ratio ( $\text{SOR} = [\text{SO}_4^{2-}]/([\text{SO}_4^{2-}] + [\text{SO}_2])$ ) and ALWC at high RH pollution condition ( $\text{RH} > 60\%$ ) (right).

In the revised manuscript lines 220-221, we added “During the polluted period, RH varied from 15% to 95% with an average value of 46% and a median value of 43%. To investigate...”.

#### Reference:

- Cerully, K. M., Bougiatioti, A., Hite Jr., J. R., Guo, H., Xu, L., Ng, N. L., Weber, R., and Nenes, A.: On the link between hygroscopicity, volatility, and oxidation state of ambient and water-soluble aerosols in the southeastern United States, *Atmos. Chem. Phys.*, 15, 8679–8694, <https://doi.org/10.5194/acp-15-8679-2015>, 2015.
- Cheng, Y. F., Zheng, G. J., Wei, C., Mu, Q., Zheng, B., Wang, Z. B., Gao, M., Zhang, Q., He, K. B., Carmichael, G., Pöschl, U., and Su, H.: Reactive nitrogen chemistry in aerosol water as a source of sulfate during haze events in China, *Sci. Adv.*, 2, e1601530, <https://doi.org/10.1126/sciadv.1601530>, 2016.
- Elser, M., Huang, R. J., Wolf, R., Slowik, J. G., Wang, Q., Canonaco, F., Li, G., Bozzetti, C., Daellenbach, K. R., Huang, Y., Zhang, R., Li, Z., Cao, J., Baltensperger, U., El-Haddad, I., and Prévôt, A. S. H.: New insights into PM2.5 chemical composition and sources in two major cities in China during extreme haze events using aerosol mass spectrometry, *Atmos. Chem. Phys.*, 16, 3207–3225, <https://doi.org/10.5194/acp-16-3207-2016>, 2016.
- Gunthe, S. S., Rose, D., Su, H., Garland, R. M., Achtert, P., Nowak, A., Wiedensohler, A., Kuwata, M., Takegawa, N., Kondo, Y., Hu, M., Shao, M., Zhu, T., Andreae, M. O., and Pöschl, U.: Cloud condensation nuclei (CCN) from fresh and aged air pollution in the megacity region of

- Beijing, *Atmos. Chem. Phys.*, 11, 11023–11039, 2011.
- Guo, H., Xu, L., Bougiatioti, A., Cerully, K.M., Capps, S.L., Hite, J.R., Jr, Carlton, A.G., Lee, S.H., Bergin, M.H., Ng, N.L.: Fine-particle water and pH in the southeastern United States, *Atmos. Chem. Phys.*, 15, 5211–5228, 2015.
- Hu, W., Hu, M., Hu, W., Jimenez, J. L., Yuan, B., Chen, W., Wang, M., Wu, Y., Chen, C., Wang, Z., Peng, J., Zeng, L., and Shao, M.: Chemical composition, sources, and aging process of submicron aerosols in Beijing: Contrast between summer and winter, *J. Geophys. Res. Atmos.*, 121(4), 1955–1977, <https://doi.org/10.1002/2015JD024020>, 2016.
- Hu, W., Hu, M., Hu, W.-W., Zheng, J., Chen, C., Wu, Y., and Guo, S.: Seasonal variations in high time-resolved chemical compositions, sources, and evolution of atmospheric submicron aerosols in the megacity Beijing, *Atmos. Chem. Phys.*, 17, 9979–10000, <https://doi.org/10.5194/acp-17-9979-2017>, 2017.
- Li, H., Zhang, Q., Zhang, Q., Chen, C., Wang, L., Wei, Z., Zhou, S., Parworth, C., Zheng, B., Canonaco, F., Prévôt, A. S. H., Chen, P., Zhang, H., Wallington, T. J., and He, K.: Wintertime aerosol chemistry and haze evolution in an extremely polluted city of the North China Plain: significant contribution from coal and biomass combustion, *Atmos. Chem. Phys.*, 17, 4751–4768, <https://doi.org/10.5194/acp-17-4751-2017>, 2017.
- Sun, Y. L., Wang, Z. F., Du, W., Zhang, Q., Wang, Q. Q., Fu, P. Q., Pan, X., Li, J., Jayne, J., and Worsnop, D. R.: Long-term real-time measurements of aerosol particle composition in Beijing, China: seasonal variations, meteorological effects, and source analysis, *Atmos. Chem. Phys.*, 15, 10149–10165, <https://doi.org/10.5194/acp-15-10149-2015>, 2015.
- Xu, W. Q., Han, T. T., Du, W., Wang, Q. Q., Chen, C., Zhao, J., Zhang, Y. J., Li, J., Fu, P. Q., Wang, Z. F., Worsnop, D. R., and Sun, Y. L.: Effects of Aqueous-Phase and Photochemical Processing on Secondary Organic Aerosol Formation and Evolution in Beijing, China, *Environ. Sci. Technol.*, 51(2), 762–770, <https://doi.org/10.1021/acs.est.6b04498>, 2017.

# Contrasting sources and processes of particulate species in haze days with low and high relative humidity in wintertime Beijing

Ru-Jin Huang<sup>1,2</sup>, Yao He<sup>1</sup>, Jing Duan<sup>1</sup>, Yongjie Li<sup>3</sup>, Qi Chen<sup>4</sup>, Yan Zheng<sup>4</sup>, Yang Chen<sup>5</sup>, Weiwei Hu<sup>6</sup>, Chunshui Lin<sup>1</sup>, Haiyan Ni<sup>1</sup>, Wenting Dai<sup>1</sup>, Junji Cao<sup>1</sup>, Yunfei Wu<sup>7</sup>, Renjian Zhang<sup>7</sup>, Wei Xu<sup>1,8</sup>, Jurgita Ovadnevaite<sup>8</sup>, Darius Ceburnis<sup>8</sup>, Thorsten Hoffmann<sup>9</sup>, Colin, D. O'Dowd<sup>8</sup>

<sup>1</sup>State Key Laboratory of Loess and Quaternary Geology, Center for Excellence in Quaternary Science and Global Change, and Key Laboratory of Aerosol Chemistry and Physics, Institute of Earth and Environment, Chinese Academy of Sciences, Xi'an 710061, China

<sup>2</sup>Open Studio for Oceanic-Continental Climate and Environment Changes, Pilot National Laboratory for Marine Science and Technology (Qingdao), Qingdao 266061, China

<sup>3</sup>Department of Civil and Environmental Engineering, Faculty of Science and Technology, University of Macau, Taipa, Macau, China

<sup>4</sup>State Key Joint Laboratory of Environmental Simulation and Pollution Control, College of Environmental Sciences and Engineering, Peking University, Beijing 100871, China

<sup>5</sup>Chongqing Institute of Green and Intelligent Technology, Chinese Academy of Sciences, Chongqing 400714, China

<sup>6</sup>State Key Laboratory of Organic Geochemistry and Guangdong Key Laboratory of Environmental Protection and Resources Utilization, Guangzhou Institute of Geochemistry, Chinese Academy of Sciences, Guangzhou 510640, China

<sup>7</sup>RCE-TEA, Institute of Atmospheric Physics, Chinese Academy of Sciences, Beijing 100029, China

<sup>8</sup>School of Physics and Centre for Climate and Air Pollution Studies, Ryan Institute, National University of Ireland Galway, University Road, Galway H91CF50, Ireland

<sup>9</sup>Institute of Inorganic and Analytical Chemistry, Johannes Gutenberg University of Mainz, Duesbergweg 10-14, 55128 Mainz, Germany

*Correspondence to:* Ru-Jin Huang (rujin.huang@ieecas.cn)

## Abstract

Although there are many studies of particulate matter (PM) pollution in Beijing, the sources and processes of secondary PM species during haze periods remain unclear. Limited studies have investigated the PM formation in highly-polluted environments under low and high relative humidity (RH) conditions. Herein, we present a systematic comparison of species in submicron particles (PM<sub>1</sub>) in wintertime Beijing (29 December 2014 to 28 February 2015) for clean periods and pollution periods under low and high RH conditions. PM<sub>1</sub> species were measured with an aerosol chemical species monitor (ACSM) and an aethalometer. Sources and processes for organic aerosol (OA) were resolved by positive matrix factorization (PMF) with multilinear engine 2 (ME-2). The comparisons for clean, low-RH pollution, and high-RH pollution periods are made from three different aspects, namely (a) mass concentration, (b) mass fraction, and (c) growth rate in diurnal profiles. OA is the dominant component of PM<sub>1</sub> with an average mass

concentration of  $56.7 \mu\text{g m}^{-3}$  (46%) during high-RH pollution and  $67.7 \mu\text{g m}^{-3}$  (54%) during low-RH pollution periods. Sulfate had higher concentration and mass fraction during high-RH pollution periods, while nitrate had higher concentration and mass fraction during low-RH pollution periods. The diurnal variations of nitrate and oxygenated organic aerosol (OOA) showed a daytime increase of their concentrations during all three types of periods. Nitrate had similar growth rates during low-RH ( $0.40 \mu\text{g m}^{-3} \text{h}^{-1}$ ) and high-RH ( $0.55 \mu\text{g m}^{-3} \text{h}^{-1}$ ) pollution periods. OOA had a higher growth rate during low-RH pollution periods ( $1.0 \mu\text{g m}^{-3} \text{h}^{-1}$ ) than during high-RH pollution periods ( $0.40 \mu\text{g m}^{-3} \text{h}^{-1}$ ). In contrast, sulfate had a decreasing trend during low-RH pollution periods, while it increased significantly with a growth rate of  $0.81 \mu\text{g m}^{-3} \text{h}^{-1}$  during high-RH pollution periods. These distinctions in mass concentrations, mass fractions, and daytime growth rates may be explained by the difference in the formation processes, affected by meteorological conditions. In particular, photochemical oxidation and aqueous-phase processes may both produce sulfate and nitrate. The relative importance of the two pathways, however, differs under different meteorological conditions. Additional OOA formation under high-RH (>70%) conditions suggests aqueous-related formation pathways. This study provides a general picture of the haze formation in Beijing under different meteorological conditions.

## 1 Introduction

Air pollution is a serious environmental problem in China, particularly in the North China Plain (NCP) in winter, affecting air quality and human health. Beijing is one of the most polluted megacities in the NCP, with an annual mean concentration of  $\text{PM}_{2.5}$  being 86 and  $51 \mu\text{g m}^{-3}$  in 2014 and 2018, respectively (<http://sthjj.beijing.gov.cn/>), which significantly exceeded the Chinese National Ambient Air Quality Standard (annual average of  $35 \mu\text{g m}^{-3}$ ). Fine PM pollution in polluted urban environments is complex and is typically associated with enhanced primary emissions from multiple sources, strong secondary aerosol formation, and stagnant weather conditions (Sun et al., 2011; 2013; 2016; Huang et al., 2014; Hu et al., 2016; An et al., 2019). Regional transport of air pollutants from urbanized and industrialized areas has an important contribution to fine PM pollution in the NCP region. For example, severe fine PM pollution in Beijing during winter often happened when prevailing air masses were from the south (Sun et al., 2016).

Organic aerosol (OA) is the major constituent of fine PM and is much less understood compared to inorganic aerosol in terms of their chemical nature and sources (Hallquist et al., 2009; Shrivastava et al., 2017). OA is composed of a wide variety of organic species from different sources, and its emission sources and atmospheric processes are not well understood so far, especially in those regions with high fine PM pollution. OA is either directly emitted to the atmosphere (primary organic aerosol, POA) or formed in the atmosphere (secondary organic aerosol, SOA). Therefore, it is essential to identify and quantify the major emission sources and understand the formation processes of OA.

The Aerodyne aerosol chemical speciation monitor (ACSM) with quadrupole (Q) or time-

of-flight (TOF) mass analyzer is capable of real-time determination of non-refractory components in submicron aerosol (NR-PM<sub>1</sub>), overcoming the limitation of filter measurements such as limited time resolution or measurement artifacts (Ng et al., 2011a; Froehlich et al., 2013). ACSM has been widely used for fine PM studies in many sites in China including Beijing, Nanjing, Shijiazhuang, and Baoji (Sun et al., 2014; Wang et al., 2017; Zhang et al., 2017; Huang et al., 2019). By applying positive matrix factorization (PMF, Paatero et al., 1993) or multilinear engine (ME-2, Canonaco et al., 2013) solver to the ACSM data, main OA sources can be identified. Those sources include hydrocarbon-like OA (HOA), biomass burning OA (BBOA), cooking OA (COA), coal combustion OA (CCOA) and oxygenated OA (OOA). OOA can further be resolved into semi-volatile OOA (SV-OOA) and low-volatility OOA (LV-OOA) by volatility, or more-oxidized OOA (MO-OOA) and less-oxidized OOA (LO-OOA) by oxidation state. MO-OOA and LO-OOA together were found to contribute 61% of OA in Beijing during summer in 2011 (Sun et al., 2012), while POA was found to be more important during winter of the same year (Sun et al., 2013). However, many recent studies show large contributions of SOA in wintertime Beijing (Huang et al., 2014; Hu et al., 2016; Xu et al., 2018) and CCOA is often found to be a large fraction of POA during wintertime pollution days in Beijing (Sun et al., 2016b; Wang et al., 2015; Elser et al., 2016). The discrepancies in SOA contribution in different measurement periods reflect the difference in atmospheric and meteorological conditions, e.g., atmospheric oxidative capacity and relative humidity (RH) (Sun et al., 2013; Xu et al., 2017; Wu et al., 2018; Song et al., 2019).

Despite the observations of large production of secondary aerosol during haze events, the formation mechanisms are not yet well understood. Specifically, more studies are needed to elucidate the relative importance of photochemical oxidation versus aqueous-phase processes on the formation of secondary aerosol during wintertime haze episodes of different meteorological conditions. In this study, we present measurement results at an urban site in Beijing during the winter of 2014-2015. The chemical nature of NR-PM<sub>1</sub>, sources of OA, formation processing of secondary aerosol in different episodes, and particularly the effects of RH on secondary aerosol formation are discussed.

## 2 Methods

### 2.1 Site description and instrumentation

The online measurements were conducted on the rooftop of a building (about 20 m above the ground level) at the campus of the National Centre for Nanoscience and Technology (40.00° N, 116.38° E) from 29 December 2014 to 28 February 2015. The observation site is between the 4<sup>th</sup> and 5<sup>th</sup> ring roads in the northwest of Beijing and is surrounded by a residential area.

A Q-ACSM was deployed for the mass concentration measurements of NR-PM<sub>1</sub> species, and the detailed operation principles can be found in Ng et al. (2011a). Briefly, ambient air was pumped through a 3/8 in stainless steel tube at a flow rate of 3 L min<sup>-1</sup>, of which 85 mL min<sup>-1</sup> was sampled into the Q-ACSM. In order to remove coarse particles, an URG

cyclone (URG-2000-30ED, size cut-off 2.5  $\mu\text{m}$ ) was installed in front of the inlet. Because particle bounce can affect collection efficiency (CE), to reduce this uncertainty and to dry the particles, a Nafion dryer (MD-110-48S; Perma Pure, Inc., Lakewood, NJ, USA) was installed after the URG cyclone. An aerodynamic lens was used to focus the submicron particles into a narrow beam, the particles beam then impinged on a heated tungsten surface (about 600  $^{\circ}\text{C}$ ) to evaporate, impacted by 70-eV electron to ionize, and then detected by a quadrupole mass spectrometer. During this study, the scan rate of Q-ACSM was at 200 ms  $\text{amu}^{-1}$  from  $m/z$  10 to 150 and the time resolution was 30 min. To determine the response factor (RF), a differential mobility analyzer (DMA, TSI model 3080) and a condensation particle counter (CPC, TSI model 3772) were used to select and count the monodisperse 350-nm ammonium nitrate ( $\text{NH}_4\text{NO}_3$ ) particles, respectively. The mass of  $\text{NH}_4\text{NO}_3$  particles was calculated with known particle size and number concentrations. This calculated mass concentration was compared to the RF of the Q-ACSM, resulting in the ionization efficiency (IE) value (Ng et al., 2011a).

The gaseous species including  $\text{O}_3$ ,  $\text{NO}_x$ , and  $\text{SO}_2$  were measured by a Thermo Scientific Model 49i ozone analyzer, a Thermo Scientific Model 42i  $\text{NO}-\text{NO}_2-\text{NO}_x$  analyzer, and an Ecotech EC 9850 sulfur dioxide analyzer, respectively. The  $\text{NH}_3$  concentrations were measured by an  $\text{NH}_3$  analyzer (Picarro G2103). The concentrations of black carbon (BC) was determined by an aethalometer (Model AE-33, Magee Scientific) with a time resolution of 1 min. In brief, light attenuation at seven different wavelengths was recorded for particle-laden filter spots, and BC concentration was retrieved based on the light attenuation at 880 nm. An automatic weather station (MAWS201, Vaisala, Vantaa, Finland) was used to measure the meteorological parameters including temperature, pressure, relative humidity and visibility, and a wind sensor (Vaisala Model QMW101-M2) was used to measure the wind speed and wind direction.

## 2.2 Data analysis

### 2.2.1 ACSM data analysis

The standard Q-ACSM data analysis software (v.1.5.3.5) written in Igor Pro (WaveMetrics, Inc., OR, USA) was used to calculate the mass concentrations for different species in  $\text{NR-PM}_{10}$ . Default relative ionization efficiencies (RIE) were used for organics (1.4), nitrate (1.1) and chloride (1.4), respectively (Ng et al., 2011a). RIE of 5.8 for ammonium and 1.2 for sulfate were determined by the IE calibrations of ammonium nitrate and ammonium sulfate. Meanwhile, data were corrected for the particle collection efficiency (CE), due to particle bounce on the vaporizer. CE can be affected by relative humidity, mass fraction of ammonium nitrate and particle acidity. In our measurement, the particles were generally neutral and dried before sampling into the ACSM. CE was calculated as  $\text{CE}_{\text{dry}} = \max(0.45, 0.0833 + 0.9167 \times \text{ANMF})$ , where ANMF refers to the ammonium nitrate fraction in  $\text{NR-PM}_{10}$  (Middlebrook et al. 2012).

### 2.2.2 OA source apportionment



The receptor model PMF using a multilinear engine (ME-2) was used to identify and quantify the OA sources. PMF is a bilinear receptor model used to describe the variability of a multivariate dataset,  $X$ , as the linear combination of a set of constant factor profiles,  $F$ , and their corresponding time series  $G$ , as expressed in equation 1.

$$X = GF + E \quad (1)$$

where  $X$  is the measured OA mass spectra consisting of  $i$  rows and  $j$  columns, and  $E$  is the model residuals. The PMF uses a least squares method to minimize the object function  $Q$ , defined as the sum of the squared residuals ( $e_{ij}$ ) weighted by their respective uncertainties ( $\sigma_{ij}$ ).

$$Q = \sum_{i=1}^m \sum_{j=1}^n (e_{ij}/\sigma_{ij})^2 \quad (2)$$

Unconstrained PMF analyses of OA data suffer from rotational ambiguity when sources show similar profiles and temporal covariation (Canonaco et al., 2013; Huang et al., 2019). However, by introducing *a priori* information as additional model input and constraining one or more output factor profiles to a predetermined range, ME-2 can overcome such difficulties and provide more environmentally meaningful solutions. When an element of a factor profile ( $f_j$ , where  $j$  refers to the  $m/z$ ) is constrained with a certain  $a$  value ( $a$ ), the following conditions need to be fulfilled:

$$f_{j,solution} = f_j \pm a \times f_j \quad (3)$$

The  $a$  value can vary between 0 and 1, which is the extent to which the output profiles can vary from the model inputs. The data analysis were conducted using the source finder (SoFi, Canonaco et al., 2013) tool version 4.9 for Igor Pro. Due to rotational ambiguity, there was no mathematically unique solution. Therefore, criteria including chemical fingerprint of the factor profiles, correlations with external tracers, and diurnal cycles were used for the factor identification and interpretation (Ulbrich et al., 2009; Huang et al., 2014; Elser et al., 2016).

### 2.2.3 Aerosol liquid water content

NR-PM<sub>1</sub> inorganic species, NH<sub>3</sub> concentrations and meteorological parameters including temperature and RH were used to calculate the aerosol liquid water content from inorganic species (ALWC<sub>i</sub>) based on the ISORROPIA-II model (Fountoukis and Nenes, 2007). Here we ran the ISORROPIA-II in “forward” mode and the particles were assumed to be deliquescent, i.e., in metastable mode (Hennigan et al., 2015). The thermodynamic equilibrium of the NH<sub>4</sub><sup>+</sup>-SO<sub>4</sub><sup>2-</sup>-NO<sub>3</sub><sup>-</sup>-Cl-H<sub>2</sub>O system was then modeled and ALWC<sub>i</sub> was calculated.

Meanwhile, the contribution of organics to ALWC (ALWC<sub>o</sub>) was also calculated using the following equation (Guo et al., 2015; Cheng et al., 2016):

$$W_{\text{org}} = \frac{\text{OM}}{\rho_{\text{org}}} \cdot \rho_w \cdot \frac{\kappa_{\text{org}}}{(100\%/\text{RH} - 1)}$$

where OM is the mass concentration of organics,  $\rho_w$  is the density of water and  $\rho_{\text{org}}$  is the density of organics ( $\rho_{\text{org}} = 1.4 \times 10^3 \text{ kg m}^{-3}$ , Cerully et al., 2015).  $\kappa_{\text{org}}$  is the hygroscopicity parameter of organic aerosol composition. We adopted a  $\kappa_{\text{org}}$  value of 0.06 based on previous cloud condensation nuclei measurements in Beijing (Gunthe et al., 2011).

## 3 Results and discussion

### 3.1 Temporal variations and mass fractions of PM<sub>1</sub> species

Fig. 1 shows the time series of mass concentrations of OA, SO<sub>4</sub><sup>2-</sup>, NO<sub>3</sub><sup>-</sup>, NH<sub>4</sub><sup>+</sup>, Cl<sup>-</sup>, and BC, as well as the meteorological parameters. The average mass concentration of PM<sub>1</sub> during the entire measurement period was 73.8  $\mu\text{g m}^{-3}$ , similar to those observed in Beijing in winter 2011 (66.8  $\mu\text{g m}^{-3}$ , Sun et al., 2013) and winter 2013 (64.0  $\mu\text{g m}^{-3}$ , Sun et al., 2016). The lowest daily average concentration was 5.2  $\mu\text{g m}^{-3}$  on 31 December, while the highest was 210.1  $\mu\text{g m}^{-3}$  on 15 January, with a difference of a factor of  $\sim 40$ . OA (52%) was the most abundant component of PM<sub>1</sub>, irrespective of the meteorological conditions, followed by nitrate (14%) and sulfate (11%). The weather conditions during the measurement period were characterized by drastic changes in wind speed, wind direction, RH and temperature, providing a unique setting to investigate the influence of meteorological conditions on PM species. The clean and pollution episodes occurred alternately during the measurement period, and the PM<sub>1</sub> concentration was usually lower than 20  $\mu\text{g m}^{-3}$  during clean episodes and higher than 100  $\mu\text{g m}^{-3}$  during pollution episodes. As such, the measurements can be divided into the clean period (PM<sub>1</sub> < 20  $\mu\text{g m}^{-3}$ ) and the pollution period (PM<sub>1</sub> > 100  $\mu\text{g m}^{-3}$ ). South/southeasterly wind directions with low speed (average, 0.9–1.0 m s<sup>-1</sup>) were typical for the pollution period, while north/northwesterly with high speed (average, 2.5 m s<sup>-1</sup>) for the clean period (Table Fig. 1).

During the polluted period, RH varied from 15% to 95% with an average value of 46% and a median value of 43%. To investigate the effects of RH on PM pollution formation, we further divided the pollution period into two categories, the low-RH pollution days (RH < 50%) and the high-RH pollution days (RH > 50%). The diurnal variations of mass concentrations and fractions of different chemical species during clean days, low-RH pollution days and high-RH pollution days are shown in Fig. 2. The mass fractional variations were flatter during low-RH and high-RH pollution days than during clean days, likely due to the accumulation of pollutants during stagnant weather conditions in pollution days. During clean days, secondary inorganic aerosol showed generally increasing trends from 06:00 to 20:00 local time (LT), despite the development of the boundary layer height during the day. The growth rate of nitrate mass (0.21  $\mu\text{g m}^{-3} \text{ h}^{-1}$ ) was higher than that of sulfate (0.04  $\mu\text{g m}^{-3} \text{ h}^{-1}$ ) and ammonium (0.10  $\mu\text{g m}^{-3} \text{ h}^{-1}$ ), indicating that formation of nitrate was perhaps faster than that of sulfate and ammonium during clean days. During low-RH pollution days, nitrate increased from 06:00 to 20:00 LT, with a growth rate of 0.40  $\mu\text{g m}^{-3} \text{ h}^{-1}$ , which was two times higher than that during clean days.

On the contrary, sulfate concentrations increased from 06:00 to 10:00 LT, then started decreasing and reached the minimum at 14:00 LT, possibly due to the increase of the boundary layer height during the day, which outweighed the production of sulfate. Associated with both sulfate and nitrate, ammonium showed a minor increase from 06:00 to 20:00 LT with a mass growth rate of  $0.18 \mu\text{g m}^{-3} \text{h}^{-1}$ . This phenomenon suggested that the low-RH condition was favorable for nitrate formation but not for sulfate formation under polluted conditions. In contrast, obvious increases of secondary inorganic species from 8:00 to 16:00 LT were observed during high-RH pollution days, with growth rates of  $0.81 \mu\text{g m}^{-3} \text{h}^{-1}$ ,  $0.55 \mu\text{g m}^{-3} \text{h}^{-1}$  and  $0.46 \mu\text{g m}^{-3} \text{h}^{-1}$  for sulfate, nitrate and ammonium, respectively. These mass growth rates increased correspondingly by about 20, 2.6 and 4.6 times compared to those during clean days. Note that nitrate growth rate in high-RH pollution days ( $0.55 \mu\text{g m}^{-3} \text{h}^{-1}$ ) was still slightly higher than that in low-RH pollution days ( $0.40 \mu\text{g m}^{-3} \text{h}^{-1}$ ), indicating that nitrate production is still efficient when RH is high, although not as much higher compared to sulfate. Measurements of sulfate oxygen isotopes suggest that the largely enhanced formation of sulfate is associated with efficient aqueous-phase reactions during high-RH pollution days (Shao et al., 2019). Note that the comparison of growth rates was done under the assumption that chemical processes were the main reason for mass growth, which might not be the case if other factors such as planetary boundary layer height variations dominate. Yet comparison of growth rates of different species in the same time period would not be affected by these factors because those species should share the same effects.

### 3.2 Sources and diurnal variations of OA

Source apportionment was performed on the OA data. Three to seven factors were examined using an unconstrained PMF model, and the factors were qualitatively identified based on their mass spectral profiles and correlation with external data. We found that a solution of five factors (i.e., HOA, COA, CCOA, BBOA, and OOA) best explains our data. For the solutions with less than 5 factors, HOA appeared to be mixed with COA while CCOA mixed with BBOA (Fig. S1). However, when the number of factors was increased to 6, the OOA factor split into two OOA factors of similar time series (Fig. S2), suggesting that further separation of the factors does not improve the interpretation of the data.

Although five factors with different profiles and temporal variations were identified by the unconstrained PMF model, the factor profiles and time series were suboptimal, specifically for HOA, COA, and BBOA. The diurnal pattern of HOA showed pronounced peaks at cooking time, indicating its mixing with COA. The fractional contribution of  $m/z$  60 ( $f_{60}$ , typically related to the fragmentation of anhydrous sugars) in HOA (0.008) was higher than the average value reported from multiple ambient datasets (0.002, Ng et al., 2011). To reduce the mixing between factors, the reference HOA mass spectral profile, characterized by a small  $f_{60}$  (Wang et al., 2017), and the BBOA mass spectral profile, derived from Beijing wintertime measurements (Elser et al., 2016), were constrained using ME-2. For the COA mass spectral profile that was derived from our unconstrained PMF analysis, a-value of 0 was used. Meanwhile, for HOA and BBOA, the  $a$  values were

varied systematically between 0 and 1 with an interval of 0.1 to explore the solution space. To assess the obtained solutions, we have set thresholds for the highest acceptable  $f_{60}$  value (0.006) for HOA and  $f_{57}$  value (0.042) for BBOA, based on mass spectra obtained at multiple sites (mean  $\pm 2\sigma$ , Ng et al., 2011). Only solutions that conform to both criteria were selected and the final solution was the average of those selected reasonable solutions (Fig. S3).

The final OA factors resolved by ME-2 include four POA (i.e., HOA, COA, BBOA and CCOA), and one SOA (i.e., OOA) factors, on average accounting for 14%, 14%, 10%, 32% and 31% of OA mass concentration, respectively. The mass spectral profiles and time series of the resolved factors are shown in Fig. 3a and b, respectively. The diurnal patterns of these factors are presented in Fig. 4. The HOA spectrum is similar to those derived from other studies in Beijing (Hu et al., 2016; Sun et al., 2014; 2016) and Pittsburgh (Ulbrich et al., 2016), and also resembles the source profile from diesel exhausts (Canagaratna et al., 2004). A strong correlation between the time series of HOA and BC was observed ( $R^2=0.84$ ). The diurnal cycle of HOA was similar to those observed in other studies in Beijing (Sun et al., 2011; 2013; 2014), showing higher mass concentrations during the night than during the day, due to enhanced traffic emissions from heavy duty vehicles and diesel trucks that are allowed to enter the inner city during the night.

Similar to HOA, the mass spectrum of COA also displayed high signals in odd fragments, while the  $m/z$  55/57 ratio (1.45) and  $m/z$  41/43 ratio (1.6) were significantly higher compared to those of the HOA factor profile ( $m/z$  55/57=0.65,  $m/z$  41/43=0.88). The COA profile is similar to those resolved in previous studies in Beijing (Elser et al., 2016; Sun et al., 2016), Paris (Crippa et al., 2013) and Zurich (Dey et al., 2004). The  $R^2$  between COA and  $m/z$  55 time series was 0.73. The diurnal cycle of COA showed two prominent peaks during lunch (12:00-13:00 LT) and dinner (18:00-19:00 LT) times, and the peak in the evening was more pronounced than that at noon, consistent with a previous study in Beijing (Sun et al., 2016). Furthermore, the diurnal variation of COA was more obvious with much clear noon and evening peaks during clean days than during low-RH and high-RH pollution days, likely because the stagnant meteorological conditions during pollution days facilitated the accumulation of pollutants and thus weakened the diurnal fluctuation.

The BBOA mass spectrum showed a similar pattern as that extracted from Crippa et al. (2014), with pronounced peaks at  $m/z$  60 and 73, two distinct markers of biomass burning emissions (Lanz et al., 2007). BBOA also showed similar time series with a high signal at  $m/z$  60 ( $R^2=0.74$ ). The diurnal cycle of BBOA showed a slight increase during the night (18:00-24:00 LT), corresponding to nighttime burning for residential heating in clean days, while this diurnal cycle became much flat during low-RH and high-RH pollution days, likely due to the stagnant meteorological conditions during pollution days. On average, BBOA contributed 10% of the total OA, much less than that of CCOA (32%), consistent with previous results in Beijing (Elser et al., 2016).

The profile of CCOA showed a moderate correlation with that resolved in Beijing in winter

2014 (Elser et al., 2016). Similar to previous studies, signals related to unsaturated hydrocarbons, especially those at  $m/z$  77, 91 and 115, contributed significantly to the total CCOA signal. In addition, there was a strong correlation between CCOA and  $\text{Cl}^-$  ( $R^2=0.82$ ), which was considered as a marker mainly from coal combustion emissions. The mass concentration and mass fraction of CCOA were both significantly higher at night than those during the day, which was observed both in clean days and pollution days. The diurnal pattern suggests much stronger emissions from coal combustion at night, a situation further deteriorated by a shallower boundary layer at night.

One secondary OA factor, namely OOA, was also resolved, characterized by an important contribution at  $m/z$  44. The profile of OOA is also similar to those resolved in Ng et al. (2011) and Sun et al. (2013). OOA is correlated well with nitrate ( $R^2=0.89$ ), and the diurnal cycle of OOA shows an increase from about 6:00 to 20:00 LT, indicating the contribution from photochemical production and accumulation of OOA. Note that the growth rate of OOA during low-RH pollution days ( $1.0 \mu\text{g m}^{-3} \text{h}^{-1}$ ) was higher than that during high-RH pollution days ( $0.40 \mu\text{g m}^{-3} \text{h}^{-1}$ ) and clean days ( $0.35 \mu\text{g m}^{-3} \text{h}^{-1}$ ) (Fig. 4).

### 3.3 Chemically resolved PM pollution

Fig. 5 shows the mass fraction of  $\text{PM}_{10}$  and OA during clean, low-RH and high-RH pollution periods. OA was the dominant component in  $\text{PM}_{10}$ , with an average concentration increasing from  $10.9 \mu\text{g m}^{-3}$  during clean periods to  $56.7 \mu\text{g m}^{-3}$  during high-RH pollution periods and further to  $67.7 \mu\text{g m}^{-3}$  during low-RH pollution periods. The corresponding mass fraction of OA was 56%, 46%, and 54%, respectively. The decrease of OA mass fraction during pollution periods can be attributed to the increased formation of sulfate and nitrate, as demonstrated in the above section. Specifically, nitrate increased from 11% ( $2.2 \mu\text{g m}^{-3}$ ) during clean periods to 14% ( $17.2 \mu\text{g m}^{-3}$ ) during high-RH pollution periods and to 15% ( $18.8 \mu\text{g m}^{-3}$ ) during low-RH pollution periods, while sulfate increased from 10% ( $2.0 \mu\text{g m}^{-3}$ ) during clean periods to 17% ( $20.9 \mu\text{g m}^{-3}$ ) during high-RH pollution periods but decreased back to as low as 7% ( $8.8 \mu\text{g m}^{-3}$ ) during low-RH pollution periods. The increased formation of nitrate from clean to pollution periods, especially during low-RH pollution periods, is likely due to enhanced photochemical production, as discussed in Lu et al. (2019) which shows fast photochemistry during wintertime haze events in Beijing. Specifically, the atmospheric oxidation proxy ( $\text{O}_x=\text{O}_3+\text{NO}_2$ ) increased from 39.2 ppb during clean periods to 47.8 ppb during high-RH pollution periods, and up to as high as 59.8 ppb during low-RH pollution periods. Meanwhile, the precursor gas for nitrate,  $\text{NO}_2$ , increased accordingly from 16.7 ppb during clean periods to ~~64.3~~42.2 ppb during high-RH pollution periods and to ~~103.0~~55.4 ppb during low-RH pollution periods. The averaged  $\text{PM}_{10}$  concentrations during high-RH ( $123.2 \mu\text{g m}^{-3}$ ) and low-RH ( $125.4 \mu\text{g m}^{-3}$ ) pollution periods were very similar, but a distinct difference lies in the sulfate and nitrate fractions in these two types of pollution periods. We observed similar a much larger contributions from nitrate during low-RH pollution periods ~~than during and~~ high-RH pollution periods, ~~which may be due to enhanced photochemical formation and also contributions of  $\text{N}_2\text{O}_5$  uptake, and while~~ a much larger contribution from sulfate during

high-RH pollution periods than during low-RH pollution periods because of enhanced formation from aqueous-phase processes.

In terms of OA sources, CCOA and OOA were the major sources irrespective of the PM<sub>1</sub> level. The mass fraction of CCOA in OA increased from 25% (2.8  $\mu\text{g m}^{-3}$ ) during clean periods to 31% (17.6  $\mu\text{g m}^{-3}$ ) during high-RH pollution periods and to 35% (23.7  $\mu\text{g m}^{-3}$ ) during low-RH pollution periods, indicating the [importance of residential coal combustion emissions during haze pollution in wintertime Beijing \(Elser et al., 2016; Li et al., 2017\)](#). OOA also increased significantly during pollution periods, from 4.1  $\mu\text{g m}^{-3}$  to  $\sim 20 \mu\text{g m}^{-3}$ . It should be noted that the average OOA mass concentrations were rather similar during high-RH (19.8  $\mu\text{g m}^{-3}$ ) and low-RH (18.3  $\mu\text{g m}^{-3}$ ) pollution periods. However, the OOA mass fraction in OA during the high-RH pollution period (35%) is higher than that during the low-RH pollution period (27%), indicating an additional contribution of OOA from e.g., aqueous-phase oxidations during high RH condition, as discussed below. The mass fraction of HOA in OA increased from 8% (0.8  $\mu\text{g m}^{-3}$ ) during clean days to 13% (8.8  $\mu\text{g m}^{-3}$ ) during low-RH pollution days and further to 16% (9.1  $\mu\text{g m}^{-3}$ ) during high-RH pollution days, suggesting an increased contribution of HOA in pollution days. The mass fraction of HOA is similar to those measured in wintertime Beijing in 2011 (14%, Hu et al., 2016) and in 2013 (11%, Sun et al., 2016). In contrast, the mass concentrations of COA during low-RH pollution days (8.8  $\mu\text{g m}^{-3}$ ) and high-RH pollution days (6.8  $\mu\text{g m}^{-3}$ ) were higher than that during clean days (2.0  $\mu\text{g m}^{-3}$ ), but the mass fraction of COA in OA during high-RH pollution days (12%) and low-RH pollution days (13%) were lower than that during clean days (20%). A similar decrease of HOA contribution and increase of COA contribution during clean days were also observed by Sun et al. (2016) in wintertime Beijing in 2011. The highest contribution of BBOA was observed during low-RH pollution days with a mass fraction of 12% (8.1  $\mu\text{g m}^{-3}$ ). The BBOA concentration during high-RH pollution days (3.4  $\mu\text{g m}^{-3}$ ) was higher than that during clean days (1.0  $\mu\text{g m}^{-3}$ ), but the mass fraction of BBOA in OA during high-RH pollution days (6%) was lower than that during clean days (10%).

The chemical composition and sources of PM<sub>1</sub> under different meteorological conditions (e.g., wind direction, wind speed and RH) in the seven pollution episodes (PM<sub>1</sub> >100  $\mu\text{g m}^{-3}$ ) and seven clean episodes (PM<sub>1</sub> <20  $\mu\text{g m}^{-3}$ ) are shown in Fig. S4. Note that these episodes in total accounted for 91% of the entire measurement period. The pollution episodes were found to be associated with the air masses from south/southwest, while clean episodes were associated with the air masses from north/northwest. Meanwhile, the pollution episodes were generally associated with higher RH and lower wind speeds when compared to the clean episodes. The wind speeds were approximately three times higher in clean episodes than those in pollution episodes. For example, the lowest concentration of PM<sub>1</sub> was 6.7  $\mu\text{g m}^{-3}$  in C6 period, corresponding to the highest wind speed (4.0 m s<sup>-1</sup>) and the lowest concentrations (< 20 ppb) of inorganic gaseous precursors (SO<sub>2</sub>, NH<sub>3</sub>, and NO<sub>x</sub>), while the highest PM<sub>1</sub> concentration of 169.0  $\mu\text{g m}^{-3}$  was found at P5, corresponding to a much lower wind speed (<1.0 m s<sup>-1</sup>). The mass concentrations of OA increased from  $\sim 4.1\text{--}9.4 \mu\text{g m}^{-3}$  during clean episodes to  $\sim 44.7\text{--}85.7 \mu\text{g m}^{-3}$  during



pollution episodes. However, the contributions of OA to  $PM_1$  showed a decreasing trend from 48-59% during clean episodes to 44-57% during pollution episodes, and the corresponding contributions of secondary inorganic species increased from 29-34% ( $\sim 2.2$ - $5.5 \mu g m^{-3}$ ) to 27-47% ( $\sim 25.5$ - $62.1 \mu g m^{-3}$ ), indicating a notable production and accumulation of secondary inorganic aerosol during haze pollution episodes. In contrast, the mass concentration of OOA increased from  $\sim 1.4$ - $3.9 \mu g m^{-3}$  during clean episodes to  $\sim 10.0$ - $27.6 \mu g m^{-3}$  during pollution episodes, while the contribution of OOA to OA decreased from 33-64% during clean episodes to 20-52% during pollution episodes. The corresponding contribution of POA sources increased from 35-67% ( $\sim 1.2$ - $4.7 \mu g m^{-3}$ ) to 38-80% ( $\sim 13.9$ - $58.7 \mu g m^{-3}$ ), suggesting that in general the emission and accumulation of POA sources played an important role during haze pollution in this measurement campaign.

Comparing the pollution episodes with different RH conditions (see Fig. S4), the mass fraction of sulfate was much higher during high-RH pollution episodes (P3, P6 and P7, 15-21%) than during low-RH pollution episodes (P1, P2, P4 and P5, 6-8%). OOA also showed a much higher contribution to OA during high-RH pollution events (62% for P6 and 50% for P7) than during low-RH pollution events (P1, P2, P4 and P5, 20-31%). These variations suggest the potential importance of aqueous-phase reactions on the formation of sulfate and OOA, as discussed above. Further comparison of high-RH and low-RH pollution episodes with similar  $PM$  levels (e.g., P2 and P6 with  $PM_1$  concentration of  $98.8 \mu g m^{-3}$  and  $99.6 \mu g m^{-3}$ , respectively) shows that secondary inorganic aerosol dominated  $PM_1$  at high-RH pollution episode. Similarly, as for the high-RH and low-RH pollution episodes with similar OA levels, for example, P6 ( $44.7 \mu g m^{-3}$ ) and P7 ( $46.3 \mu g m^{-3}$ ), OOA dominated the particulate pollution (62% of OA) at high-RH pollution events due to efficient formation of SOA. On the contrary, POA had increased contributions to  $PM$  pollution at low RH and stagnant weather conditions (from 38% of OA at high-RH pollution to 50% of OA at low-RH pollution), consistent with previous studies in other Chinese cities (e.g., Wang et al., 2017; Huang et al., 2019). These results indicate that meteorological conditions have important effects on the particulate pollution.

### 3.4 Formation of secondary aerosol

The relationship between  $SO_4^{2-}$  and  $NO_3^-$  is investigated to elucidate the formation processes of these two typical secondary inorganic aerosol species. The correlation between  $SO_4^{2-}$  and  $NO_3^-$  was weak for the entire pollution period, because of the varied relative contribution of different formation processes during different periods. However, better correlations between  $SO_4^{2-}$  and  $NO_3^-$  were found with different slopes when the data were divided into low-RH (RH < 50%) and high-RH (RH > 50%) pollution periods (Fig. 6). During low-RH pollution periods,  $NO_3^-$  and  $SO_4^{2-}$  showed a good correlation ( $R^2 = 0.75$ ) with a ratio of 2.1, indicating a similar photochemical production process. Meanwhile, the high ratio between  $NO_3^-$  and  $SO_4^{2-}$  suggest the nitrate production is more efficient than that of sulfate during low-RH pollution period. However, during high-RH pollution periods, the ratio of  $NO_3^-$  to  $SO_4^{2-}$  decreased significantly to 0.40 with a lower correlation coefficient

( $R^2 = 0.53$ ). The degraded temporal correlation between nitrate and sulfate suggest different formation pathway of nitrate and sulfate during high RH pollution periods. Aqueous-phase production of  $\text{SO}_4^{2-}$  become important during those periods. Consistently, Fig. 7 shows that the sulfate oxidation ratio ( $\text{SOR} = [\text{SO}_4^{2-}]/([\text{SO}_4^{2-}] + [\text{SO}_2])$ ) increased exponentially with the increase of ALWC at  $\text{RH} > 50\%$ .

A strong correlation of the mass concentrations between OOA and  $\text{NO}_3^-$  was observed with  $R^2$  of 0.84 (Fig. 8a), possibly explained by the dominant contribution of photochemical production for both OOA and  $\text{NO}_3^-$ . Meanwhile, the  $\text{O}_x$  concentration during low-RH pollution days (59.8 ppb) was higher than that during high-RH pollution days (47.8 ppb) and clean days (39.2 ppb). With the higher  $\text{O}_x$  concentration (as a surrogate of oxidant level) under low-RH conditions, the daytime formation of OOA was more efficient and the growth rate was higher during those low-RH pollution days than those during high-RH pollution days and clean days. When considering the RH effect (color coded in Fig. 8a), it is found that the data are scattered around the regression line with uniform slope when  $\text{RH} < 70\%$  but concentrated in a small area above the regression line when  $\text{RH} > 70\%$ , suggesting that the OOA formation at  $\text{RH} > 70\%$  is probably promoted by aerosol water. This is further supported by the linear increase of OOA with increasing  $\text{SO}_4^{2-}$  when  $\text{RH} > 70\%$ , while the relationship between OOA and  $\text{SO}_4^{2-}$  was very scattered when  $\text{RH} < 70\%$  (Fig. 8b).

#### 4 Conclusion

We conducted online measurements of  $\text{PM}_{10}$  in urban Beijing from 29 December 2014 to 27 February 2015. The average mass concentration of  $\text{PM}_{10}$  was  $73.8 \mu\text{g m}^{-3}$  and OA was the most important component of  $\text{PM}_{10}$  (52%), followed by nitrate (14%) and sulfate (10%). Source apportionment of OA resolved five factors including HOA, COA, BBOA, CCOA, and OOA, in which CCOA (32%) and OOA (32%) were the most important sources to OA. The mass proportion of CCOA in OA showed a significant increase from clean period (25%) to pollution periods (31-35%), highlighting the important role of coal burning in haze formation in wintertime Beijing. The meteorological conditions (WD, WS, and RH) have a significant impact on the chemical composition and evolution of  $\text{PM}_{10}$  species. Nitrate had a higher contribution during low-RH pollution days, implying the photochemical oxidation process of nitrate formation. In contrast, the mass fraction of sulfate to  $\text{PM}_{10}$  was much higher during high-RH pollution episodes compared to those during low-RH pollution episodes. The data also showed the exponential increase of sulfate oxidation ratio (SOR) with ALWC at high RH conditions. Both are consistent with the impacts of aqueous-phase reactions on the formation of sulfate. As for the OOA formation, the strong correlation between OOA and  $\text{NO}_3^-$  may be explained by the dominant role of photochemical production on both species; aqueous-phase processes may add an additional contribution to OOA formation under high RH condition, as indicated by the linear increase of OOA with increasing  $\text{SO}_4^{2-}$  when  $\text{RH} > 70\%$ . These results provide insights into the relative importance of photochemical oxidation and aqueous-phase processes for secondary aerosol formation during haze pollution, demonstrating the

significance of meteorological conditions in the formation of secondary aerosol.

*Data availability.* Raw data used in this study are archived at the Institute of Earth Environment, Chinese Academy of Sciences, and are available on request by contacting the corresponding author.

*Supplement.* The Supplement related to this article is available online at

*Competing interests.* The authors declare that they have no conflict of interest.

*Author contributions.* RJH designed the study. Data analysis and interpretation were made by YH, JD, and RJH. RJH, JD, and YH prepared the manuscript with contributions from all authors.

*Acknowledgments.* This work was supported by the National Natural Science Foundation of China (NSFC) under Grant No. 41925015, 91644219, 41877408 and 41675120, the National Key Research and Development Program of China (No. 2017YFC0212701), the Chinese Academy of Sciences (no. ZDBS-LY-DQC001, XDB40000000), and the Cross Innovative Team fund from the State Key Laboratory of Loess and Quaternary Geology (No. SKLLQGTD1801), and the Irish Environmental Protection Agency and Science Foundation Ireland project of OM-MaREI.

- Alfarra, M. R., Prévôt, A. S. H., Szidat, S., Sandradewi, J., Weimer, S., Lanz, V. A., Schreiber, D.,  
Mohr, M., and Baltensperger, U.: Identification of the mass spectral signature of organic  
aerosols from wood burning emissions, *Environ. Sci. Technol.*, 41, 5770-5777, 2007.
- An, Z., Huang, R.-J., Zhang, R., Tie, X., Li, G., Cao, J., Zhou, W., Shi, Z., Han, Y., Gu, Z., and Ji, Y.:  
Severe haze in northern China: A synergy of anthropogenic emissions and  
atmospheric processes, *Proc. Natl. Acad. Sci.*, 116(18), 8657-8666, 2019.
- Canagaratna, M. R., Jayne, J. T., Ghertner, D. A., Herndon, S., Shi, Q., Jimenez, J. L., Silva, P. J.,  
Williams, P., Lanni, T., Drewnick, F., Demerjian, K. L., Kolb, C. E., and Worsnop, D. R.:  
Chase studies of particulate emissions from in-use New York City vehicles, *Aerosol Sci.*  
*Tech.*, 38(6), 555-573, 2004.
- Canagaratna, M. R., Jayne, J. T., Jimenez, J. L., Allan, J. D., Alfarra, M. R., Zhang, Q., Onasch, T.  
B., Drewnick, F., Coe, H., Middlebrook, A., Delia, A., Williams, L. R., Trimborn, A. M.,  
Northway, M. J., DeCarlo, P. F., Kolb, C. E., Davidovits, P., and Worsnop, D. R.: Chemical  
and microphysical characterization of ambient aerosols with the Aerodyne aerosol  
mass spectrometer, *Mass Spectro. Rev.*, 26(2), 185-222, <https://doi.org/10.1002/mas.20115>, 2007.
- Canonaco, F., Crippa, M., Slowik, J. G., Baltensperger, U., and Prévôt, A. S. H.: SoFi, an IGOR-  
based interface for the efficient use of the generalized multilinear engine (ME-2) for  
the source apportionment: ME-2 application to aerosol mass spectrometer data,  
*Atmos. Meas. Tech.*, 6, 3649-3661, <https://doi.org/10.5194/amt-6-3649-2013>, 2013.
- Canonaco, F., Slowik, J. G., Baltensperger, U., and Prévôt, A. S. H.: Seasonal differences in  
oxygenated organic aerosol composition: implications for emissions sources and  
factor analysis, *Atmos. Chem. Phys.*, 15, 6993-7002, <https://doi.org/10.5194/acp-15-6993-2015>, 2015.
- Cerully, K. M., Bougiatioti, A., Hite Jr., J. R., Guo, H., Xu, L., Ng, N. L., Weber, R., and Nenes, A.:  
On the link between hygroscopicity, volatility, and oxidation state of ambient and  
water-soluble aerosols in the southeastern United States, *Atmos. Chem. Phys.*, 15,  
8679-8694, <https://doi.org/10.5194/acp-15-8679-2015>, 2015.
- Cheng, Y. F., Zheng, G. J., Wei, C., Mu, Q., Zheng, B., Wang, Z. B., Gao, M., Zhang, Q., He, K. B.,  
Carmichael, G., Pöschl, U., and Su, H.: Reactive nitrogen chemistry in aerosol water as  
a source of sulfate during haze events in China, *Sci. Adv.*, 2, e1601530,  
<https://doi.org/10.1126/sciadv.1601530>, 2016.
- Chow, J. C., Bachmann, J. D., Wierman, S. S.G., Mathai, C.V., Malm, W. C., White, W. H., Mueller,  
P. K., Kumar, N., and Watson, J. G.: Visibility: Science and Regulation, *J. Air. Waste.*  
*Manage.*, 52 (9), 973-999, 2002.
- Crippa, M., Decarlo, P. F., Slowik, J. G., Mohr, C., Heringa, M. F., Chirico, R., Poulain, L., Freutel,  
F., Sciare, J., Cozic, J., Di Marco, C. F., Elsasser, M., Nicolas, J., Marchand, Nicolas, Abidi, E.,  
Wiedensohler, A., Drewnick, F., Schneider, J., Borrmann, S., Nemitz, E., Zimmermann, R.,  
Jaffrezo, J.-L., Prévôt, A. S. H., and Baltensperger U.: Wintertime aerosol chemical  
composition and source apportionment of the organic fraction in the metropolitan  
area of Paris, *Atmos. Chem. Phys.*, 13, 961-981, <https://doi.org/10.5194/acp-13-961-2013>, 2013.

- DeCarlo, P. F., Kimmel, J. R., Trimborn, A., Northway, M. J., Jayne, J. T., Aiken, A. C., Gonin, M., Fuhrer, K., Horvath, T., Docherty, K. S., Worsnop, D. R., and Jimenez, J. L.: Field-deployable, high-resolution, time-of-flight aerosol mass spectrometer, *Anal. Chem.*, 78(24), 8281–8289, <https://doi.org/10.1021/ac061249n>, 2006.
- DeCarlo, P. F., Ulbrich, I. M., Crounse, J., de Foy, B., Dunlea, E. J., Aiken, A. C., Knapp, D., Weinheimer, A. J., Campos, T., Wennberg, P. O., and Jimenez, J. L.: Investigation of the sources and processing of organic aerosol over the Central Mexican Plateau from aircraft measurements during MILAGRO, *Atmos. Chem. Phys.*, 10, 5257–5280, <https://doi.org/10.5194/acp-10-5257-2010>, 2010.
- Deng, X., Tie, X., Wu, D., Zhou, X. J., Bi, X. Y., Tan, H. B., Li, F., and Jaing, C. L.: Long-term trend of visibility and its characterizations in the Pearl River Delta (PRD) region, China, *Atmos. Environ.*, 42(7), 1424–1435, 2008.
- Elser, M., Huang, R. J., Wolf, R., Slowik, J. G., Wang, Q., Canonaco, F., Li, G., Bozzetti, C., Daellenbach, K. R., Huang, Y., Zhang, R., Li, Z., Cao, J., Baltensperger, U., El-Haddad, I., and Prévôt, A. S. H.: New insights into PM<sub>2.5</sub> chemical composition and sources in two major cities in China during extreme haze events using aerosol mass spectrometry, *Atmos. Chem. Phys.*, 16, 3207–3225, <https://doi.org/10.5194/acp-16-3207-2016>, 2016.
- Forster, P., Ramaswamy, V., and Artaxo, P.: Changes in atmospheric constituents and in radiative forcing, Cambridge University Press: Cambridge, United Kingdom, pp 129–234, 2007.
- Goldstein, A. H., and Galbally, I. E.: Known and unexplored organic constituents in the earth's atmosphere, *Environ. Sci. Technol.*, 41 (5), 1514–1521, 2007.
- Gunthe, S. S., Rose, D., Su, H., Garland, R. M., Achtert, P., Nowak, A., Wiedensohler, A., Kuwata, M., Takegawa, N., Kondo, Y., Hu, M., Shao, M., Zhu, T., Andreae, M. O., and Poschl, U.: Cloud condensation nuclei (CCN) from fresh and aged air pollution in the megacity region of Beijing, *Atmos. Chem. Phys.*, 11, 11023–11039, 2011.
- Guo, H., Xu, L., Bougiatioti, A., Cerully, K.M., Capps, S.L., Hite, J.R., Jr, Carlton, A.G., Lee, S.H., Bergin, M.H., Ng, N.L.: Fine-particle water and pH in the southeastern United States, *Atmos. Chem. Phys.*, 15, 5211–5228, 2015.
- Hennigan, C. J., Izumi, J., Sullivan, A. P., Weber, R. J., and Nenes, A.: A critical evaluation of proxy methods used to estimate the acidity of atmospheric particles, *Atmos. Chem. Phys.*, 15, 2775–2790, <https://doi.org/10.5194/acp-15-2775-2015>, 2015.
- Hagler, G. S. W., Bergin, M. H., Salmon, L. G., Yu, J. Z., Wan, E. C. H., Zheng, M., Zeng, L. M., Kiang, C. S., Zhang, Y. H., Lau, A. K. H., and Schauer, J. J.: Source areas and chemical composition of fine particulate matter in the Pearl River Delta region of China, *Atmos. Environ.*, 40 (20), 3802–3815, 2006.
- Han, S., Kondo, Y., Oshima, N., Takegawa, N., Miyazaki, Y., Hu, M., Lin, P., Deng, Z., Zhao, Y., Sugimoto, N., and Wu, Y.: Temporal variations of elemental carbon in Beijing, *J. Geophys. Res. Atmos.*, 114, 2009.
- He, L.-Y., Huang, X.-F., Xue, L., Hu, M., Lin, Y., Zheng, J., Zhang, R., and Zhang, Y.-H.: Submicron aerosol analysis and organic source apportionment in an urban atmosphere in Pearl River Delta of China using high-resolution aerosol mass spectrometry, *J. Geophys. Res. Atmos.*, 116, D12, <https://doi.org/10.1029/2010JD014566>, 2011.

584 Hien, P. D., Bac, V. T., and Thinh, N. T. H.: PMF receptor modelling of fine and coarse PM 10,  
 585 in air masses governing monsoon conditions in Hanoi, northern Vietnam, *Atmos.*  
 586 *Environ.*, 38(2), 189-201, 2004.

587 Hu, W. W., Hu, M., Yuan, B., Jimenez, J. L., Tang, Q., Peng, J. F., Hu, W., Shao, M., Wang, M.,  
 588 Zheng, L. M., Wu, Y. S., Gong, Z. H., Huang, X. F., and He, L. Y.: Insights on organic aerosol  
 589 aging and the influence of coal combustion at a regional receptor site of central eastern  
 590 China, *Atmos. Chem. Phys.*, 13, 10095–10112, [https://doi.org/10.5194/acp-13-](https://doi.org/10.5194/acp-13-10095-2013)  
 591 10095-2013, 2013.

592 Hu, W., Hu, M., Hu, W., Jimenez, J. L., Yuan, B., Chen, W., Wang, M., Wu, Y., Chen, C., Wang, Z.,  
 593 Peng, J., Zeng, L., and Shao, M.: Chemical composition, sources, and aging process of  
 594 submicron aerosols in Beijing: Contrast between summer and winter, *J. Geophys. Res.*  
 595 *Atmos.*, 121(4), 1955–1977, <https://doi.org/10.1002/2015JD024020>, 2016.

596 Huang, R. J., Zhang, Y. L., Bozzetti, C., Ho, K. F., Cao, J. J., Han, Y. M., Daellenbach, K. R., Slowik,  
 597 J. G., Platt, S. M., Canonaco, F., Zotter, P., Wolf, R., Pieber, S. M., Bruns, E. A., Crippa, M.,  
 598 Ciarelli, G., Piazzalunga, A., Schwikowski, M., Abbaszade, G., Schnelle-Kreis, J.,  
 599 Zimmermann, R., An, Z., Szidat, S., Baltensperger, U., Haddad, I. E., and Prevot, A. S. H.:  
 600 High secondary aerosol contribution to particulate pollution during haze events in  
 601 China, *Nature*, 514, 218–222, 2014.

602 Huang, R.-J., Wang, Y., Cao, J., Lin, C., Duan, J., Chen, Q., Li, Y., Gu, Y., Yan, J., Xu, W., Fröhlich,  
 603 R., Canonaco, F., Bozzetti, C., Ovadnevaite, J., Ceburnis, D., Canagaratna, M. R., Jayne, J.,  
 604 Worsnop, D. R., El-Haddad, I., Prévôt, A. S. H., and O'Dowd, C. D.: Primary emissions  
 605 versus secondary formation of fine particulate matter in the most polluted city  
 606 (Shijiazhuang) in North China, *Atmos. Chem. Phys.*, 19, 2283–2298,  
 607 <https://doi.org/10.5194/acp-19-2283-2019>, 2019.

608 Huang, X.-F., Yu, J. Z., He, L.-Y., and Yuan, Z. B.: Water-soluble organic carbon and oxalate in  
 609 aerosols at a coastal urban site in China: Size distribution characteristics, sources, and  
 610 formation mechanisms, *J. Geophys. Res. Atmos.*, 111(D22), 2006.

611 Huang, X.-F., He, L.-Y., Hu, M., Canagaratna, M. R., Kroll, J. H., Ng, N. L., Zhang, Y.-H., Lin, Y.,  
 612 Xue, L., Sun, T.-L., Liu, X.-G., Shao, M., Jayne, J. T., and Worsnop, D. R.: Characterization  
 613 of submicron aerosols at a rural site in Pearl River Delta of China using an Aerodyne  
 614 High-Resolution Aerosol Mass Spectrometer, *Atmos. Chem. Phys.*, 11, 1865–1877,  
 615 <https://doi.org/10.5194/acp-11-1865-2011>, 2011.

616 Huang, X. F., He, L. Y., Xue, L., Sun, T. L., Zeng, L. W., Gong, Z. H., Hu, M., and Zhu, T.: Highly  
 617 time-resolved chemical characterization of atmospheric fine particles during 2010  
 618 Shanghai world expo, *Atmos. Chem. Phys.*, 12, 4897–4907, [https://doi.org/10.5194/](https://doi.org/10.5194/acp-12-4897-2012)  
 619 acp-12-4897-2012, 2012.

620 Huang, X.-F., Xue, L., Tian, X.-D., Shao, W. W., Sun, T. L., Gong, Z. H., Ju, W. W., Jiang, B., Hu, M.,  
 621 and He, L. Y.: Highly time-resolved carbonaceous aerosol characterization in Yangtze  
 622 River Delta of China: Composition, mixing state and secondary formation, *Atmos.*  
 623 *Environ.*, 64, 200-207, 2013.

624 Huffman, J. A., Docherty, K. S., Aiken, A. C., Cubison, M. J., Ulbrich, I. M., DeCarlo, P. F., Sueper,  
 625 D., Jayne, J. T., Worsnop, D. R., Ziemann, P. J., and Jimenez, J. L.: Chemically-resolved  
 626 aerosol volatility measurements from two megacity field studies, *Atmos. Chem. Phys.*,



- 9, 7161–7182, <https://doi.org/10.5194/acp-9-7161-2009>, 2009.
- Jenkin, M. E.: Investigation of an oxidant-based methodology for AOT40 exposure assessment in the UK, *Atmos. Environ.*, 94, 332–340, 2014.
- Jimenez, J. L., Jayne, J. T., Shi, Q., Kolb, C. E., Worsnop, D. R., Yourshaw, I., Seinfeld, J. H., Flagan, R. C., Zhang, X., Smith, K. A., Morris, J. W., and Davidovits, P.: Ambient aerosol sampling with an Aerosol Mass Spectrometer, *J. Geophys. Res.-Atmos.*, 108, 8425, doi:10.1029/2001JD001213, 2003.
- Jimenez, J. L., Canagaratna, M. R., Donahue, N. M., Prevot, A. S. H., Zhang, Q., Kroll, J. H., DeCarlo, P. F., Allan, J. D., Coe, H., Ng, N. L., Aiken, A. C., Docherty, K. S., Ulbrich, I. M., Grieshop, A. P., Robinson, A. L., Duplissy, J., Smith, J. D., Wilson, K. R., Lanz, V. A., Hueglin, C., Sun, Y. L., Tian, J., Laaksonen, A., Raatikainen, T., Rautiainen, J., Vaattovaara, P., Ehn, M., Kulmala, M., Tomlinson, J. M., Collins, D. R., Cubison, M. J., Dunlea, J., Huffman, J. A., Onasch, T. B., Alfarra, M. R., Williams, P. I., Bower, K., Kondo, Y., Schneider, J., Drewnick, F., Borrmann, S., Weimer, S., Demerjian, K., Salcedo, D., Cottrell, L., Griffin, R., Takami, A., Miyoshi, T., Hatakeyama, S., Shimojo, A., Sun, J. Y., Zhang, Y. M., Dzepina, K., Kimmel, J. R., Sueper, D., Jayne, J. T., Herndon, S. C., Trimborn, A. M., Williams, L. R., Wood, E. C., Middlebrook, A. M., Kolb, C. E., Baltensperger, U., and Worsnop, D. R.: Evolution of organic aerosols in the atmosphere, *Science*, 326, 1525–1529, <https://doi.org/10.1126/science.1180353>, 2009.
- Kadowaki, S.: On the nature of atmospheric oxidation processes of sulfur dioxide to sulfate and of nitrogen dioxide to nitrate on the basis of diurnal variations of sulfate, nitrate, and other pollutants in an urban area, *Environ. Sci. Technol.*, 20(12), 86–93, 1986.
- Kanakidou, M., Seinfeld, J. H., Pandis, S. N., Barnes, I., Dentener, F. J., Facchini, M. C., Van Dingenen, R., Ervens, B., Nenes, A., Nielsen, C. J., Swietlicki, E., Putaud, J. P., Balkanski, Y., Fuzzi, S., Horth, J., Moortgat, G. K., Winterhalter, R., Myhre, C. E. L., Tsigaridis, K., Vignati, E., Stephanou, E. G., and Wilson, J.: Organic aerosol and global climate modelling: a review, *Atmos. Chem. Phys.*, 5, 1053–1123, <https://doi.org/10.5194/acp-5-1053-2005>, 2005.
- Khoder, M. I.: Atmospheric conversion of sulfur dioxide to particulate sulfate and nitrogen dioxide to particulate nitrate and gaseous nitric acid in an urban area, *Chemosphere*, 49(6), 675–84, 2002.
- Lanz, V. A., Alfarra, M. R., Baltensperger, U., Buchmann, B., Hueglin, C., and Prévôt, A. S. H.: Source apportionment of submicron organic aerosols at an urban site by factor analytical modelling of aerosol mass spectra, *Atmos. Chem. Phys.*, 7, 1503–1522, <https://doi.org/10.5194/acp-7-1503-2007>, 2007.
- Lanz, V. A., Prévôt, A. S. H., Alfarra, M. R., Weimer, S., Mohr, C., DeCarlo, P. F., Gianini, M. F. D., Hueglin, C., Schneider, J., Favez, O., D'Anna, B., George, C., and Baltensperger, U.: Characterization of aerosol chemical composition with aerosol mass spectrometry in Central Europe: an overview, *Atmos. Chem. Phys.*, 10, 10453–10471, <https://doi.org/10.5194/acp-10-10453-2010>, 2010.
- Lee, B. P., Li, Y. J., Yu, J. Z., Louie, P. K. K., and Chan, C. K.: Characteristics of submicron particulate matter at the urban roadside in downtown Hong Kong Overview of 4 months of continuous high-resolution aerosol mass spectrometer measurements, *J. Geophys. Res.-Atmos.*, 120 (14), 7040–7058, 2015.

- Li, H., Zhang, Q., Zhang, Q., Chen, C., Wang, L., Wei, Z., Zhou, S., Parworth, C., Zheng, B., Canonaco, F., Prévôt, A. S. H., Chen, P., Zhang, H., Wallington, T. J., and He, K.: Wintertime aerosol chemistry and haze evolution in an extremely polluted city of the North China Plain: significant contribution from coal and biomass combustion, *Atmos. Chem. Phys.*, **17**, 4751–4768, <https://doi.org/10.5194/acp-17-4751-2017>, 2017.
- Li, Y. J., Lee, B. P., Su, L., Fung, J. C. H., and Chan, C. K.: Seasonal characteristics of fine particulate matter (PM) based on high resolution time-of-flight aerosol mass spectrometric (HR-ToF AMS) measurements at the HKUST Supersite in Hong Kong, *Atmos. Chem. Phys.*, **15**, 37–53, <https://doi.org/10.5194/acp-15-37-2015>, 2015.
- Lu, K., Fuchs, H., Hofzumahaus, A., Tan, Z., Wang, H., Zhang, L., Schmitt, S. H., Rohrer, F., Bohn, B., Broch, S., Dong, H., Gkatzelis, G. I., Hohaus, T., Holland, F., Li, X., Liu, Y., Ma, X., Novelli, A., Schlag, P., Shao, M., Wu, Y., Wu, Z., Zeng, L., Hu, M., Kiendler-Scharr, A., Wahner, A., and Zhang, Y.: Fast Photochemistry in Wintertime Haze: Consequences for Pollution Mitigation Strategies, *Environ. Sci. Technol.*, **53**(18), 10676–10684, 2019.
- Massoli, P., Fortner, E. C., Canagaratna, M. R., Williams, L. R., Zhang, Q., Sun, Y. L., Schwab, J. J., Trimborn, A., Onasch, T. B., Demerjian, K. L., Kolb, C. E., Worsnop, D. R., and Jayne, J. T.: Pollution Gradients and Chemical Characterization of Particulate Matter from Vehicular Traffic Near Major Roadways: Results from the 2009 Queens College Air Quality Study in NYC, *Aerosol Sci. Technol.*, **46**, 1201–1218, doi:10.1080/02786826.2012.701784, 2012.
- Matson, P., Lohse, K. A., and Hall, S. J.: The globalization of nitrogen deposition: Consequences for terrestrial ecosystems, *Ambio*, **31** (2), 113–119, 2002.
- Murphy, J. G., Day, D. A., and Cleary, P. A.: The weekend effect within and downwind of Sacramento – Part 1: Observations of ozone, nitrogen oxides, and VOC reactivity, *Atmos. Chem. Phys.*, **7**(20), 5327–5339, 2007.
- Nilsson, P. T., Eriksson, A. C., Ludvigsson, L., Messing, M. E., Nordin, E. Z., Gudmundsson, A., Meuller, B. O., Deppert, K., Fortner, E. C., Onasch, T. B., and Pagels, J. H.: In-situ characterization of metal nanoparticles and their organic coatings using laser-vaporization aerosol mass spectrometry, *Nano Research*, **8** (12), 3780–3795, 2015.
- Ng, N. L., Herndon, S. C., Trimborn, A., Canagaratna, M. R., Croteau, P. L., Onasch, T. B., Sueoer, D., Worsnop, D. R., Zhang, Q., Sun, Y. L., and Jayne, J. T.: An Aerosol Chemical Speciation Monitor (ACSM) for routine monitoring of the composition and mass concentrations of ambient aerosol, *Aerosol Sci. Technol.*, **45** (7), 770–784, <https://doi.org/10.1080/02786826.2011.560211>, 2011a.
- Ng, N. L., Canagaratna, M. R., Jimenez, J. L., Zhang, Q., Ulbrich, M., and Worsnop, D. R.: Real-time methods for estimating organic component mass concentrations from aerosol mass spectrometer data, *Environ. Sci. Technol.*, **45**, 910–916, <https://doi.org/10.1021/es102951k>, 2011b.
- Paatero, P., and Tapper, U.: Positive matrix factorization: A non-negative factor model with optimal utilization of error estimates of data values, *Environmetrics*, **5** (2), 111–126, 1994.
- Peng, R. D., Dominici, F., Pastor-Barriuso, R., Zeger, S. L., and Samet, J. M.: Seasonal analyses of air pollution and mortality in 100 US cities, *Am. J. Epidemiol.*, **161** (6), 585–594, 2005.
- Pope, C. A., Burnett, R. T., Thun, M. J., Calle, E. E., Krewski, D., Ito, K., and

- Thurston, G. D.: Lung cancer, cardiopulmonary mortality, and long-term exposure to fine particulate air pollution, *J. Am. Med. Assoc.*, 287, 1132–1141, 2002.
- Pudasainee, D., Sapkota, B., Bhatnagar, A., Kim, S. H., and Seo, Y. C.: Influence of weekdays, weekends and bandhas on surface ozone in Kathmandu valley, *Atmos. Res.*, 95(2–3), 150–156, 2010.
- Schauer, J. J., Rogge, W. F., Hildemann, L. M., Mazurek, M. A., Cass, G. R., and Simoneit, B. R.: Source apportionment of airborne particulate matter using organic compounds as tracers, *Atmos. Environ.*, 30 (22), 3837–3855, 1996.
- Schneider, J., Weimer, S., Drewnick, F., Borrmann, S., Helas, G., Gwaze, P., Schmid, O., Andreae, M.O. and Kirchner, U.: Mass spectrometric analysis and aerodynamic properties of various types of combustion-related aerosol particles, *Int. J. Mass. Spectrom.*, 258(1–3), 37–49, 2006.
- Seinfeld, J. H., Pandis, S. N., and Noone, K.: Atmospheric chemistry and physics: from air pollution to climate change, *Physics Today*, 51, 88, 1998.
- Shao, J., Chen, Q., Wang, Y., Lu, X., He, P., Sun, Y., Shah, V., Martin, R. V., Philip, S., Song, S., Zhao, Y., Xie, Z., Zhang, L., and Alexander, B.: Heterogeneous sulfate aerosol formation mechanisms during wintertime Chinese haze events: air quality model assessment using observations of sulfate oxygen isotopes in Beijing, *Atmos. Chem. Phys.*, 19, 6107–6123, <https://doi.org/10.5194/acp-19-6107-2019>, 2019.
- Song, S., Nenes, A., Gao, M., Zhang, Y., Liu, P., Shao, J., Ye, D., Xu, W., Lei, L., Sun, Y., Liu, B., Wang, S., and McElroy, M.: Thermodynamic modeling suggests declines in water uptake and acidity of inorganic aerosols in Beijing winter haze events during 2014/2015–2018/2019, *Environ. Sci. & Tech. Let.*, 6(12), 752–760, 2019.
- Sun, C., Lee, B. P., Huang, D., Jie Li, Y., Schurman, M. I., Louie, P. K. K., Luk, C., and Chan, C. K.: Continuous measurements at the urban roadside in an Asian megacity by Aerosol Chemical Speciation Monitor (ACSM): particulate matter characteristics during fall and winter seasons in Hong Kong, *Atmos. Chem. Phys.*, 16, 1713–1728, <https://doi.org/10.5194/acp-16-1713-2016>, 2016.
- Sun, Y. L., Zhang, Q., Schwab, J. J., Demerjian, K. L., Chen, W. N., Bae, M. S., Hung, H. M., Hogrefe, O., Frank, B., Rattigan, O. V., and Lin, Y. C.: Characterization of the sources and processes of organic and inorganic aerosols in New York city with a high-resolution time-of-flight aerosol mass spectrometer, *Atmos. Chem. Phys.*, 11, 1581–1602, [doi:10.5194/acp-11-1581-2011](https://doi.org/10.5194/acp-11-1581-2011), 2011.
- Sun, Y. L., Wang, Z., Dong, H., Yang, T., Li, J., Pan, X., Chen, P., and Jayne, J. T.: Characterization of summer organic and inorganic aerosols in Beijing, China with an Aerosol Chemical Speciation Monitor, *Atmos. Environ.*, 51, 250–259, [doi:10.1016/j.atmosenv.2012.01.013](https://doi.org/10.1016/j.atmosenv.2012.01.013), 2012.
- Sun, Y. L., Wang, Z. F., Fu, P. Q., Yang, T., Jiang, Q., Dong, H. B., Li, J., and Jia, J. J.: Aerosol composition, sources and processes during wintertime in Beijing, China, *Atmos. Chem. Phys.*, 13, 4577–4592, <https://doi.org/10.5194/acp-13-4577-2013>, 2013.
- Sun, Y. L., Wang, Z. F., Fu, P. Q., Jiang, Q., Yang, T., Li, J., and Ge, X. L.: The impact of relative humidity on aerosol composition and evolution processes during wintertime in Beijing, China, *Atmos. Environ.*, 77, 927–934, 2013.
- Sun, Y., Jiang, Q., Wang, Z., Fu, P., Li, J., Yang, T., and Yin, Y.: Investigation of the sources and

- evolution processes of severe haze pollution in Beijing in January 2013, *J. Geophys. Res. Atmos.*, 119, 4380–4398, <https://doi.org/10.1002/2014JD021641>, 2014.
- Sun, Y. L., Wang, Z. F., Du, W., Zhang, Q., Wang, Q. Q., Fu, P. Q., Pan, X., Li, J., Jayne, J., and Worsnop, D. R.: Long-term real-time measurements of aerosol particle composition in Beijing, China: seasonal variations, meteorological effects, and source analysis, *Atmos. Chem. Phys.*, 15, 10149–10165, <https://doi.org/10.5194/acp-15-10149-2015>, 2015.
- Sun, Y., Du, W., Fu, P., Wang, Q., Li, J., Ge, X., Zhang, Q., Zhu, C., Ren, L., Xu, W., Zhao, J., Han, T., Worsnop, D. R., and Wang, Z.: Primary and secondary aerosols in Beijing in winter: sources, variations and processes, *Atmos. Chem. Phys.*, 16, 8309–8329, <https://doi.org/10.5194/acp-16-8309-2016>, 2016.
- Ulbrich, I. M., Canagaratna, M. R., Zhang, Q., Worsnop, D. R., and Jimenez, J. L.: Interpretation of organic components from Positive Matrix Factorization of aerosol mass spectrometric data, *Atmos. Chem. Phys.*, 9, 2891–2918, <https://doi.org/10.5194/acp-9-2891-2009>, 2009.
- Vecchi, R., Marcazzan, G., Valli, G., Ceriani, M., and Antoniazzi, C.: The role of atmospheric dispersion in the seasonal variation of PM<sub>1</sub> and PM<sub>2.5</sub> concentration and composition in the urban area of Milan (Italy), *Atmos. Environ.*, 38 (27), 4437–4446, 2004.
- Wang, Y. C., Huang, R. J., Ni, H. Y., Chen, Y., Wang, Q. Y., Li, G. H., Tie, X. X., Shen, Z. X., Huang, Y., Liu, S. X., Dong, W. M., Xue, P., Fröhlich, R., Canonaco, F., Elser, M., Daellenbach, K.R., Bozzetti, C., Haddad, E.I., and Cao, J. J.: Chemical composition, sources and secondary processes of aerosols in Baoji city of northwest China, *Atmos. Environ.*, 158, 128–137, <https://doi.org/10.1016/j.atmosenv.2017.03.026>, 2017.
- Wu, Y. Z., Ge, X. L., Wang, J. F., Shen, Y. F., Ye, Z. L., Ge, S., Wu, Y., Yu, H., and Chen, M. D.: Responses of secondary aerosols to relative humidity and photochemical activities in an industrialized environment during late winter, *Atmos. Environ.*, 193, 66–78, 2018.
- Xu, W. Q., Han, T. T., Du, W., Wang, Q. Q., Chen, C., Zhao, J., Zhang, Y. J., Li, J., Fu, P. Q., Wang, Z. F., Worsnop, D. R., and Sun, Y. L.: Effects of Aqueous-Phase and Photochemical Processing on Secondary Organic Aerosol Formation and Evolution in Beijing, China, *Environ. Sci. Technol.*, 51(2), 762–770, <https://doi.org/10.1021/acs.est.6b04498>, 2017.
- Xu, W. Q., Sun, Y. L., Wang, Q. Q., Zhao, J., Wang, J. F., Ge, X. L., Xie, C. H., Zhou, W., Du, W., Li, J., Fu, P. Q., Wang, Z. F., Worsnop, D. R., and Coe, H.: Changes in aerosol chemistry from 2014 to 2016 in winter in Beijing: insights from high resolution aerosol mass spectrometry, *J. Geophys. Res. Atmos.*, 124(2), 1132–1147, 2018.
- Zhang, Q., Alfarra, M. R., Worsnop, D. R., Allan, J. D., Coe, H., Canagaratna, M. R., and Jimenez, J. L.: Deconvolution and quantification of hydrocarbon-like and oxygenated organic aerosols based on aerosol mass spectrometry, *Environ. Sci. Technol.*, 39 (13), 4938–4952, 2005.
- Zhang, Q., Jimenez, J. L., Canagaratna, M. R., Allan, J. D., Coe, H., Ulbrich, I., and Dzepina, K.: Ubiquity and dominance of oxygenated species in organic aerosols in anthropogenically-influenced Northern Hemisphere midlatitudes, *Geophys. Res. Lett.*, 34 (13), 2007.
- Zhang, Q., Meng, J., Quan, J., Gao, Y., Zhao, D., Chen, P., and He, H.: Impact of aerosol composition on cloud condensation nuclei activity, *Atmos. Chem. Phys.*, 12, 3783–

- 3790, <https://doi.org/10.5194/acp-12-3783-2012>, 2012.
- Zhang, Y., Schauer, J. J., Zhang, Y., Zeng, L., Wei, Y., Liu, Y., and Shao, M.: Characteristics of particulate carbon emissions from real-world Chinese coal combustion, *Environ. Sci. Technol.*, 42 (14), 5068-5073, 2008.
- Zhang, Y., Tang, L., Yu, H., Wang, Z., Sun, Y., Qin, W., and Ge, S.: Chemical composition, sources and evolution processes of aerosol at an urban site in Yangtze River Delta, China during wintertime, *Atmos. Environ.*, 123, 339-349, 2015a.
- Zhang, Y. J., Tang, L. L., Wang, Z., Yu, H. X., Sun, Y. L., Liu, D., and Zhou, H. C.: Insights into characteristics, sources, and evolution of submicron aerosols during harvest seasons in the Yangtze River delta region, China. *Atmos. Chem. and Phys.*, 15(3), 1331-1349.
- Zhang, Y. M., Zhang, X. Y., Sun, J. Y., Lin, W. L., Gong, S. L., Shen, X. J., and Yang, S.: Characterization of new particle and secondary aerosol formation during summertime in Beijing, China, *Tellus B.*, 63(3), 382-394, 2011.
- Zhang, Y. J., Tang, L. L., Sun, Y. L., Favez, O., Canonaco, F., Albinet, A., Couvidat, F., Liu, D. T., Jayne, J. T., Wang, Z., Croteau, P. L., Canagaratna, M. R., Zhou, H. C., Prevot, A. S. H., and Worsnop, D.R.: Limited formation of isoprene epoxydiols-derived secondary organic aerosol under NO<sub>x</sub> - rich environments in Eastern China, *Geophys. Res. Lett.*, 44(4), 2035 – 2043, <https://doi.org/10.1002/2016GL072368>, 2017.
- Zheng, B., Zhang, Q., Zhang, Y., He, K. B., Wang, K., Zheng, G. J., Duan, F. K., Ma, Y. L., and Kimoto, T.: Heterogeneous chemistry: a mechanism missing in current models to explain secondary inorganic aerosol formation during the January 2013 haze episode in North China, *Atmos. Chem. Phys.*, 15, 2031–2049, <https://doi.org/10.5194/acp-15-2031-2015>, 2015.

**Table1** Summary of the PM<sub>1</sub> composition, OA sources and meteorological conditions during different pollution periods.

Species	Clean	High-RH pollution	Low-RH pollution
PM <sub>1</sub> (μg m <sup>-3</sup> )	19.5	123.2	125.4
Org (μg m <sup>-3</sup> )	10.9 (56%)	56.7 (46%)	67.7 (54%)
SO <sub>4</sub> <sup>2-</sup> (μg m <sup>-3</sup> )	2.0 (10%)	20.9 (17%)	8.8 (7%)
NO <sub>3</sub> <sup>-</sup> (μg m <sup>-3</sup> )	2.2 (11%)	17.2 (14%)	18.8 (15%)
NH <sub>4</sub> <sup>+</sup> (μg m <sup>-3</sup> )	1.8 (9%)	12.3 (10%)	11.3 (9%)
Cl <sup>-</sup> (μg m <sup>-3</sup> )	1.0 (5%)	7.4 (6%)	8.8 (7%)
BC (μg m <sup>-3</sup> )	1.7 (9%)	8.6 (7%)	10.0 (8%)
HOA (μg m <sup>-3</sup> )	0.8 (8%)	9.1 (16%)	8.8 (13%)
COA (μg m <sup>-3</sup> )	2.0 (20%)	6.8(12%)	8.8 (13%)
BBOA (μg m <sup>-3</sup> )	1.0 (10%)	3.4 (6%)	8.1 (12%)
CCOA (μg m <sup>-3</sup> )	2.8 (25%)	17.6 (31%)	23.7 (35%)
OOA (μg m <sup>-3</sup> )	4.1 (37%)	19.8 (35%)	18.3 (27%)
O <sub>x</sub> (ppb)	39.2	47.8	59.8
NO <sub>2</sub> (ppb)	16.7	<del>64.3</del> 42.2	<del>103.0</del> 55.4
RH (%)	25.0	60.0	31.0
WS (m s <sup>-1</sup> )	2.5	1.0	0.9
Vis (Km)	15.7	6.5	6.7

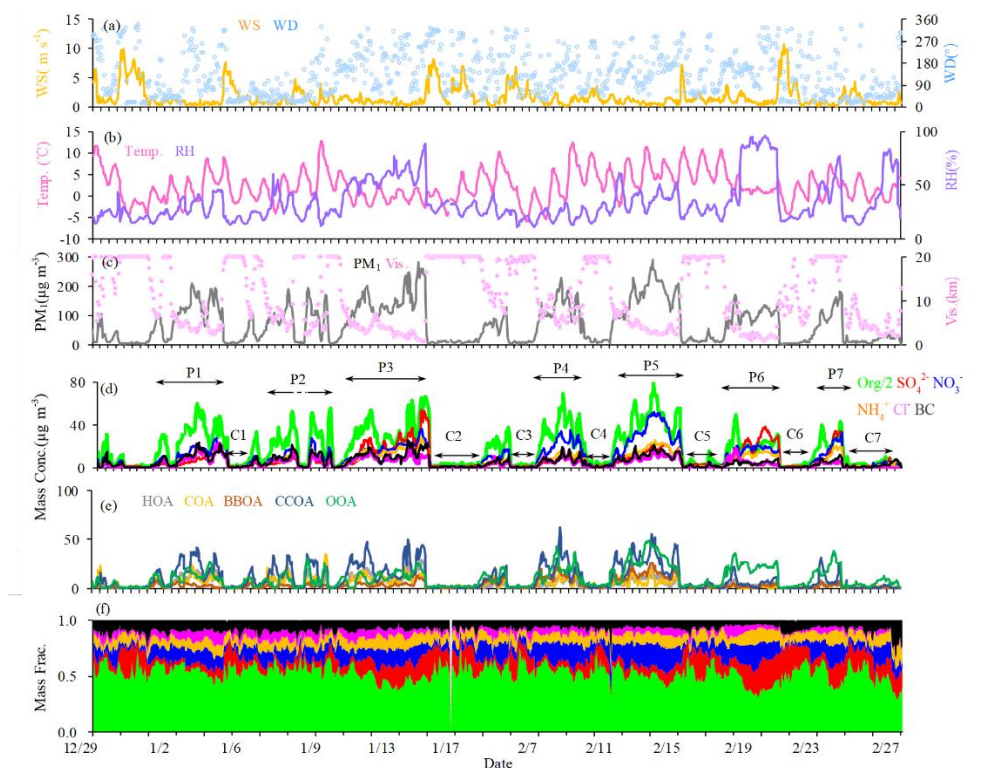
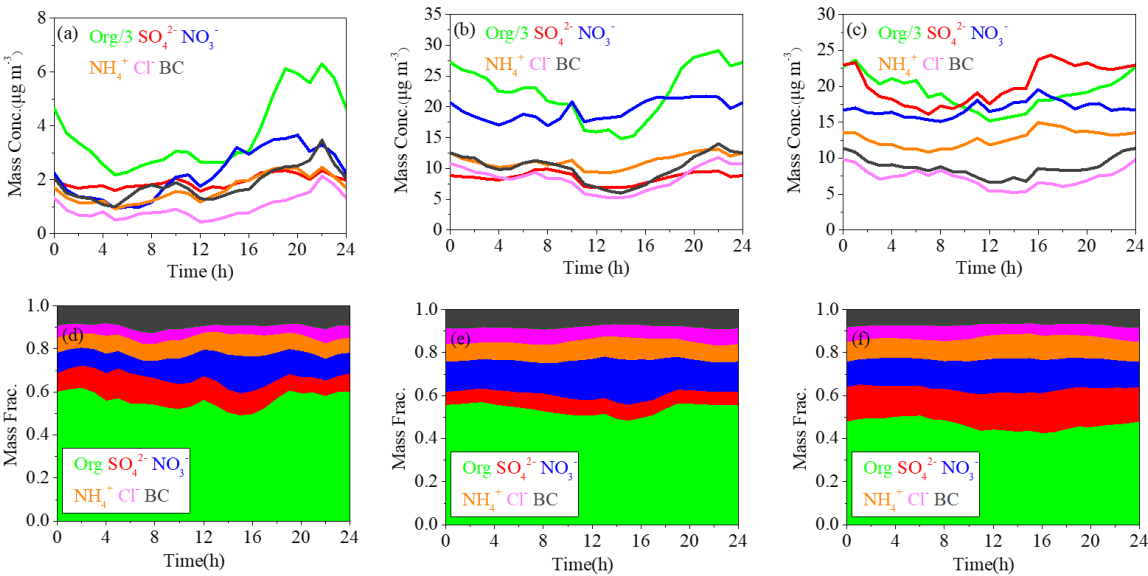


**Figure 1.** Time series of (a) wind speed (WS) and wind direction (WD), (b) Temperature (Temp) and relative humidity (RH), (c) visibility and PM<sub>1</sub>, (d) NR-PM<sub>1</sub> species (i.e., OA, SO<sub>4</sub><sup>2-</sup>, NO<sub>3</sub><sup>-</sup>, NH<sub>4</sub><sup>+</sup>, Cl<sup>-</sup> and BC; note that OA is halved clarity), (e) OA factors (i.e., HOA, COA, BBOA, CCOA and OOA), and (f) relative contribution of PM<sub>1</sub> species.





849

850 **Figure 2.** The diurnal variations of mass concentrations and relative contributions of PM<sub>1</sub>  
851 components during clean days (a, d), low-RH pollution days (b, e) and high-RH pollution  
852 days (c, f).

853

854

855

856

857

858

859

860

861

862

863

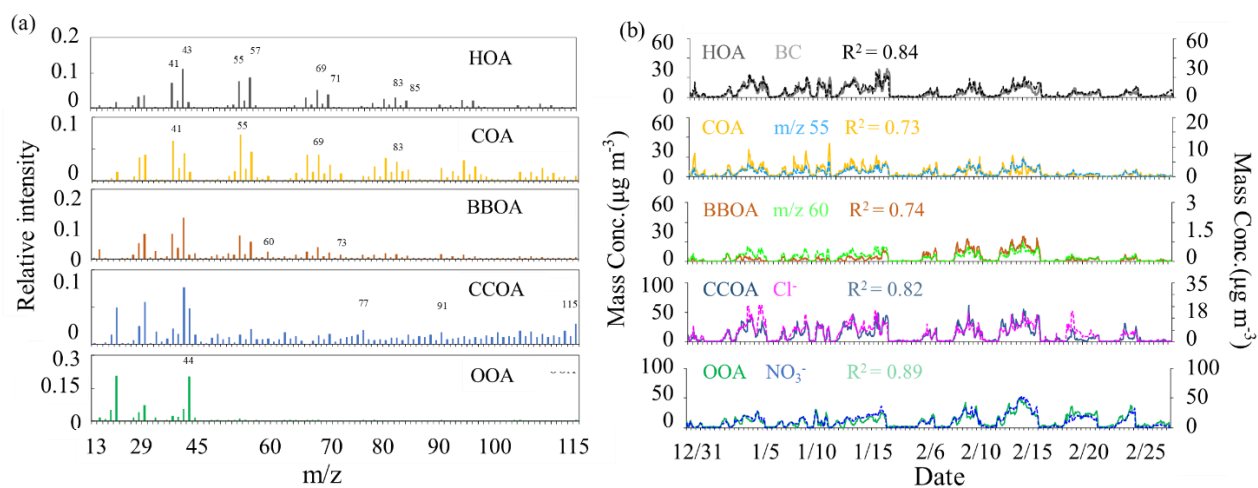
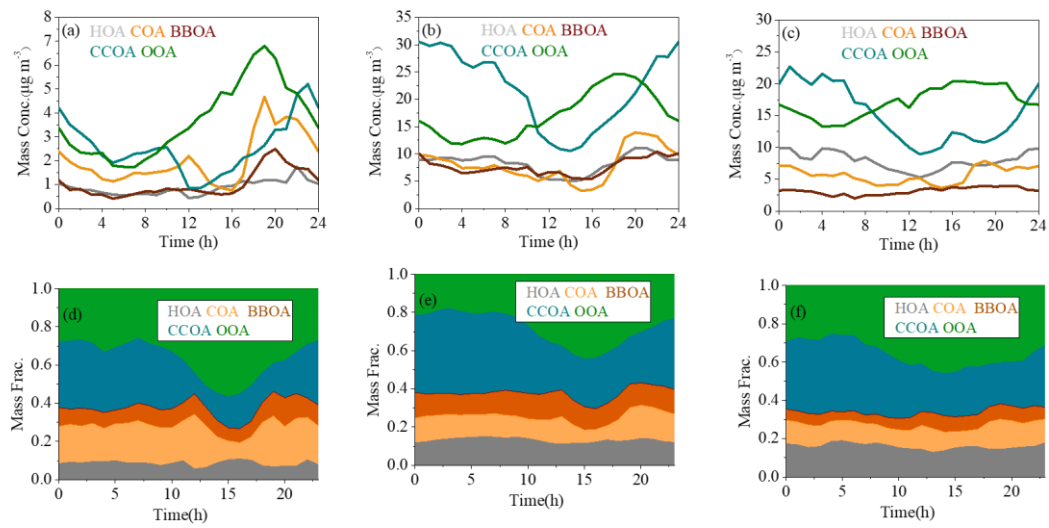


**Figure 3.** The mass spectra(a) and time series(b) of OA factors (HOA, COA, BBOA, CCOA, and OOA).

881



882

883 **Figure 4.** The diurnal variations of mass concentrations and relative contributions of OA  
884 factors during clean days (a, d), low-RH pollution days (b, e) and high-RH pollution days  
885 (c, f).

886

887

888

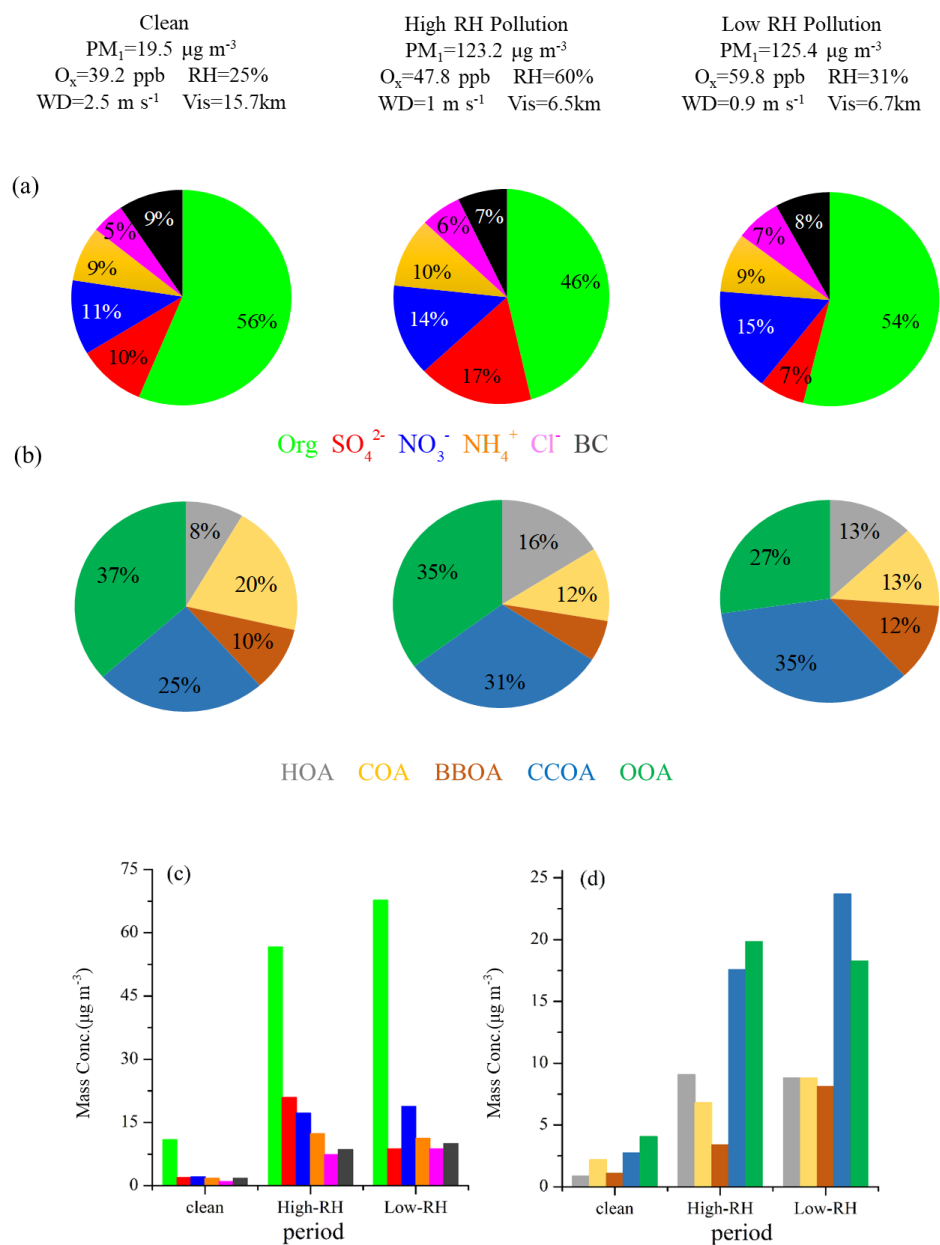


**Figure 5.** PM<sub>1</sub> chemical composition (a) and OA source composition (b) pie chart as well as the mass concentrations of PM<sub>1</sub> species(c) and OA sources(d) during clean, High-RH pollution and Low-RH pollution periods.

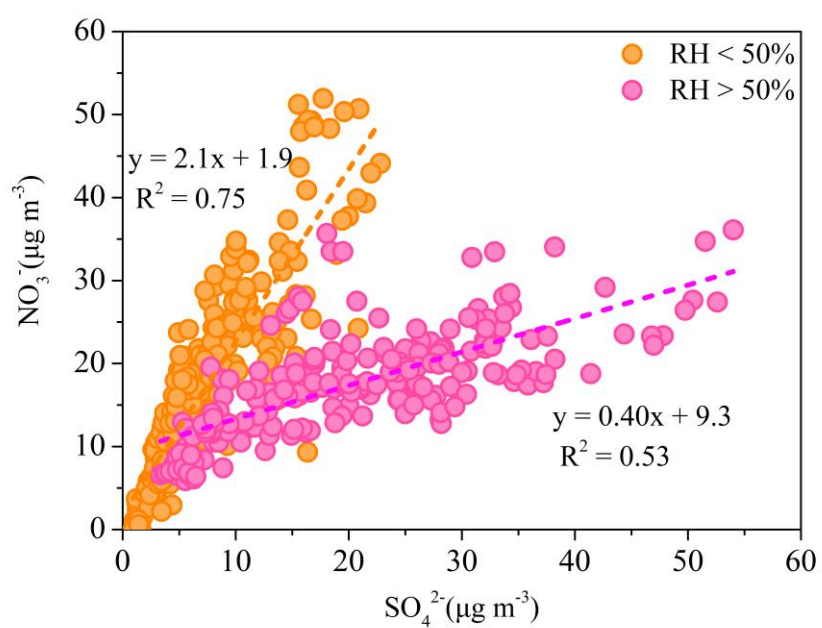


**Figure 6.** The relationship between  $\text{SO}_4^{2-}$  and  $\text{NO}_3^-$  during low-RH (RH <50%) and high-RH (RH >50%) pollution episodes.

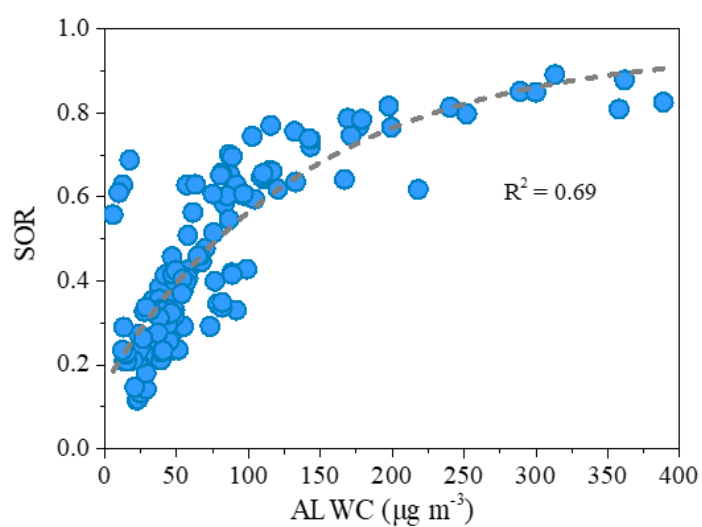


**Figure 7.** The relationship between the sulfate oxidation ratio ( $SOR = [SO_4^{2-}] / ([SO_4^{2-}] + [SO_2])$ ) and ALWC at high RH pollution condition ( $RH > 50\%$ ).

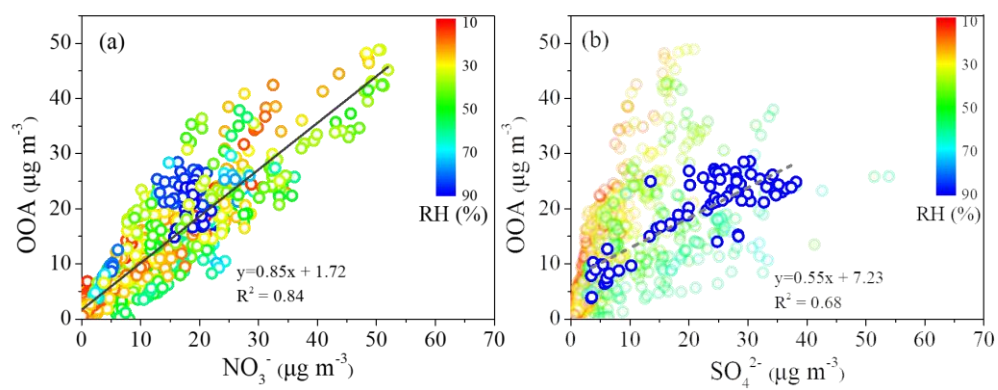


**Figure 8.** Scatter plot between the mass concentration of OOA and  $\text{NO}_3^-$  (colored by RH) (a), and scatter plot between the mass concentration of OOA and  $\text{SO}_4^{2-}$  (colored by RH) (b).